A STUDY OF
THE NATURAL FREQUENCIES OF A VIBRATING RECTANGULAR PLATE WITH POINT SUPPORTS AT EACH CORNER

A THESIS

Presented to

the Faculty of the Graduate Division

by

Thomas Ellis Adams

In Partial Fulfillment of the Requirements

for the Degree

Master of Science in Engineering Mechanics

Georgia Institute of Technology

March, 1967

A STUDY OF

THE NATURAL FREQUENCIES OF A VIBRATING RECTANGULAR PLATE WITH POINT SUPPORTS AT EACH CORNER

Approved:

Thesis Advisor

Date Approved by Chairman: 1/25/67

ACKNOWLEDGEMENT

The author wishes to thank the many persons whose combined efforts have made this thesis possible.

The author is especially indebted to Dr. Charles E. Stoneking for his guidance during the study. It was he who first suggested that this investigation be made, and he has given unselfishly of his time and effort throughout the work.

Dr. W. J. Lnenicka and Dr. H. L. Johnson of the reading committee are thanked for their helpful comments on the text.

Special thanks are also due for the assistance of the Lockheed-Georgia Company, Marietta, Georgia, and in particular, Mr. D. G. Cumro, Department Engineer, in making available the facilities for conducting the research work described in this thesis.

And last, the author would like to express his deepest appreciation to his wife and parents for their continued encouragement during this study.

TABLE OF CONTENTS

LIST OF TABLES

LIST OF ILLUSTRATIONS

NOTATION

a	1/2 length of plate
b	1/2 width of plate
h	thickness of plate
D	bending rigidity
A_{mn}	integration constants
m, n, i, j, p, q	summation indices
g	acceleration of gravity
t	time
V_{max}	amplitude of the strain energy
E	Young's modulus
L_o	$\frac{a}{b}$
T_{max}	amplitude of the kinetic energy
$W(x, y, t)$	transverse displacement
$W(x, y), w$	amplitude of $W(x, y, t)$
x, y	Cartesian coordinates
γ	weight density
ρ	mass density
K	dimensionless frequency parameter, $\dfrac{.25\,\omega}{\sqrt{\dfrac{D}{\rho h a^4}}}$
ω	angular frequency
f	linear frequency, cps
Δ	$\left[\frac{\partial^2}{\partial x^2} + \frac{\partial^2}{\partial y^2}\right]$
$[P]$	potential energy matrix
$[K]$	kinetic energy matrix
$[D]$	dynamical matrix
$[U]$	unit matrix
$\{A_{mn}\}$	coefficient column matrix
δ	Kronecker delta, vibration constant

ABSTRACT

This thesis reports the investigation of the natural frequencies of a vibrating, rectangular plate which is point-supported at each of its corners. The upper bounds of the first twelve natural frequencies were determined for both a square plate and a rectangular plate with a length-to-width ratio of 2, using the Ritz energy method. The results obtained were then compared to experimental results.

A double series deflection equation with a leading second order polynomial was used to estimate the deflection of the plates investigated. The equations were programmed and solved numerically in their final form with a computer using standard subroutines for transformations and solutions.

Two experimental plates were excited in the range of their natural frequencies with sodium chloride sprinkled over their surface. When the plates were excited at their natural frequencies, the salt accumulated in the regions of zero vibration, the nodal lines.

Results from the analytical and experimental investigations in most cases were in close agreement; however, the analytical frequency was not, in all cases, an upper bound as indicated by the Ritz theory. Furthermore, for the deflection equation assumed, the calculated frequency may be in error as much as thirty-four percent on the most important mode, the fundamental.

CHAPTER I

INTRODUCTION

The linear equation of motion for the free transverse vibration of thin rectangular plates is well known, but exact solutions have been found for only a few different sets of boundary conditions. The Ritz energy method is one of several possible methods that may be used to find approximate solutions to problems of vibrating plates with various edge conditions. Ritz calculated the frequencies of a square plate with all edges free up to the 35th mode (1). This well known, classical technique is used in this thesis to investigate the modes of vibration of thin plates with point supports at each corner. The modes predicted by these solutions have been compared with test results. The convergence and accuracy of the Ritz method has been discussed by various authors including R. Courant (2), and L. Collatz (3). It is well known that this method should yield the upper bounds of the frequencies. The major handicap of the technique is the large amount of computation required for setting up the necessary equations and for the solution of the resulting set of equations.

Theoretically, there are an infinite number of solutions to the governing differential equation

$$\Delta^2\Delta^2 w - \delta w = 0 \tag{1}$$

where $\delta = \frac{\gamma h \omega}{Dg}$. There are, therefore, an infinite number of modes of vibration for a vibrating plate. These modes are a function of the edge conditions and the geometry of the plate. B. Grinsted (4) relates how Chaldni (1787) described the irregular nodal patterns that occurred on vibrating plates by sprinkling fine sand on a vibrating specimen. The complexity of the solution was exemplified by the sand patterns formed.

Dr. Mary Waller investigated the vibrations of free circular and square plates (5, 6). So-called Chaldni figures were produced when carbon dioxide was used as a forcing function by being placed in contact with the plate to be investigated. Dr. Waller presents photographs of the patterns produced using this technique.

Cox and Boxer (7), using a finite difference method, calculated frequencies for vibrating square plates that were point-supported at each corner. This difference method was used to simplify the programming necessary for a computer solution to the problem. The variation of frequency with respect to Poisson's ratio was also presented. Frequencies up to the fifth harmonic were found for square plates, and the fundamental frequencies for plates with various length-to-width ratios were given. The authors relate that the values obtained were within one percent deviation from the experimental values.

The present problem was also investigated by N. Rajappa (8). Rajappa assumed, for the purpose of analysis, that the plate was composed of a series of interconnected beams. The results obtained for the fundamental frequency were thirty-eight percent higher than those obtained by Cox and Boxer. The fundamental frequency was the only case considered. This variation in results was attributed to the choice of the characteristic function used in the analysis.

R. E. Reed, Jr. (9) investigated the problem analytically, using an approximation to the governing differential equation in the form of a trigonometric series, and the Ritz method with an assumed deflection equation. The results of both methods were then compared to experimental results. The series solution and the experimental results yielded close correlation with the work of Cox and Boxer. The Ritz method, however, deviated as much as ten percent high. This deviation was attributed to the slow convergence of the method.

Difference calculus was used to investigate the described problem by T. Nishimura (10). His analytical results were checked with experimentation and the results agreed within three percent. The greatest deviation was the fundamental mode, and the analytical results given were approximately nine percent higher than those of Cox and Boxer.

CHAPTER II

THEORY

The complete solution of the problem of finding the natural frequencies of a vibrating plate which is point-supported at each of its corners, as shown in Figure 1, resolves itself to that of finding an exact solution of the differential equation of motion of the plate with the following conditions:

Displacements at the supports are

$$w(+a, +b) = w(-a, +b) = w(+a, -b) = w(-a, -b) = 0$$

Moments along the edges are

$$\left.\begin{aligned} \frac{\partial^2}{\partial x^2} w(\pm a, y) + \nu \frac{\partial^2}{\partial x^2} w(\pm a, y) &= 0 \\ \frac{\partial^2}{\partial y^2} w(x, \pm b) + \nu \frac{\partial^2}{\partial y^2} w(x, \pm b) &= 0 \end{aligned}\right\} \qquad (2)$$

An approximate solution may be found through the use of the well known method of Ritz. The Ritz method may be carried out as follows. First, a solution is assumed in the form of a series which satisfies the boundary conditions but which has undetermined parameters A_i. These functions are inserted into the expressions for both the potential energy and the kinetic energy and the required integrations are then performed. The resulting expressions are functions of the undetermined parameters A_i, where $i = 1, 2, \ldots, n$ and the natural frequency.

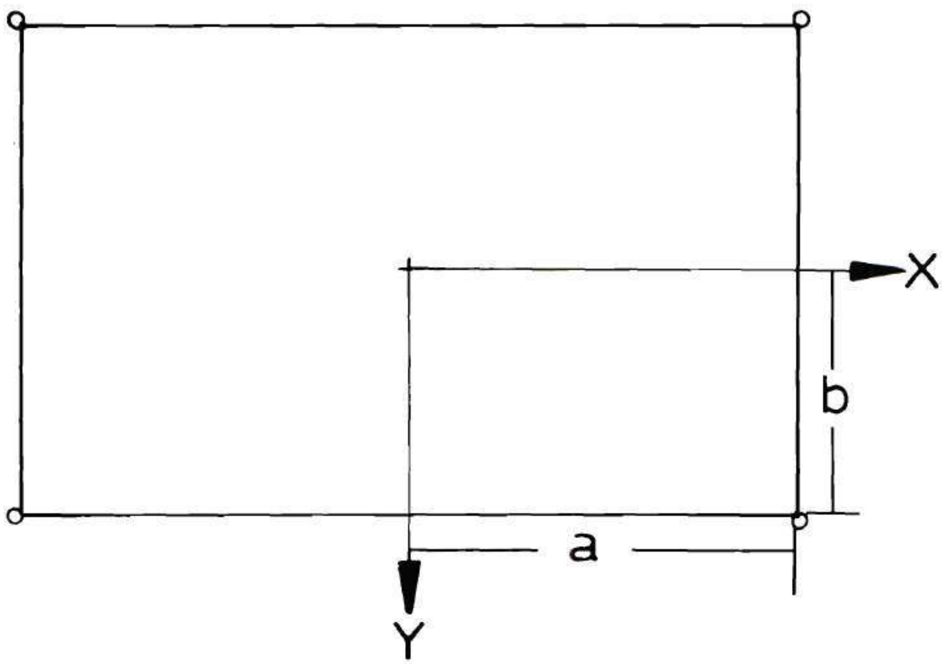

Fiqure 1. Plate Coordinate System

Since the sum of the potential and kinetic energies must be constant at all times in the vibrating system, either the undetermined parameters, A_i, or the natural frequencies can be obtained by minimizing the total energy expression with respect to each A_i. If n parameters are taken, then n simultaneous equations are found. The function

$$W(x, y, t) = w(x, y) \cos \omega t \tag{3}$$

was used to approximate the solution to the present problem subject to the following assumptions:

1. The deflections of the plate are small in comparison with the thickness of the plate.
2. The bending effects of the shearing forces are considered negligible.
3. The neutral surface of the plate coincides with the middle surface of the plate.
4. The cross sections of the plate remain plane during bending.
5. The plate is assumed to be a perfectly elastic, homogeneous, isotropic material with a uniform thickness, h, that is small in comparison with the other dimensions.
6. The function w(x, y) is a series of "admissible" functions.

For the functions of w(x, y) to be "admissible" each term of the series chosen must satisfy the boundary conditions of the deflections. It need not satisfy the requirements of the shear and the moment (11). Of course, a more rapid convergence is assured should the function w(x, y) also satisfy these latter boundary conditions.

The displacement was represented by

$$w(x, y) = h\left[2 - \frac{x^2}{a^2} - \frac{y^2}{b^2}\right] \sum_{m=1}^{\infty} \sum_{n=1}^{\infty} A_{mn} \left[\frac{x}{a}\right]^m \left[\frac{y}{b}\right]^n \tag{4}$$

Note that each of the functions of (4) satisfies the deflection requirements. For a uniform plate which is vibrating harmonically with amplitude w(x, y) and circular frequency ω, the maximum potential energy is given by

$$V_{max} = 2D \int_0^a \int_0^b \left[\left[\frac{\partial^2 w}{\partial x^2}\right]^2 + \left[\frac{\partial^2 w}{\partial y^2}\right]^2 + 2\nu\left[\frac{\partial^2 w \partial^2 w}{\partial x^2 \partial y^2}\right] + 2(1 - \nu)\left[\frac{\partial^2 w}{\partial x \partial y}\right]^2\right] dxdy \tag{5}$$

and the maximum kinetic energy is

$$T_{max} = \frac{2\gamma h\omega^2}{g} \int_0^a \int_0^b w^2 dxdy \tag{6}$$

Since the motion is harmonic, then

$$V_{max} = T_{max} \tag{7}$$

Solving for ω^2 after substitution of (5) and (6) in (7) yields

$$\omega^2 = \frac{g\,V_{max}}{2h\gamma \int_0^a \int_0^b w^2 dxdy} \tag{8}$$

When w(x, y), as given by equation (4), is substituted in (8), the right side becomes a function of the coefficients A_{mn}. The Ritz method then requires that (8) be minimized by taking the partial derivative with respect to each coefficient A_{mn} and equating to zero. The resulting system of linear homogeneous equations will be of the form

$$\frac{\partial}{\partial A_{ij}} V_{max} - \frac{2\omega^2 h\gamma}{g} \frac{\partial}{\partial A_{ij}} \int_0^a \int_0^b w^2 dxdy = 0 \tag{9}$$

where A_{ij} is any one of the coefficients A_{mn}. These equations in matrix form appear as

$$\left[\left[P \right] - \left[K \right] \omega^2 \right] \left\{ A_{mn} \right\} = 0 \tag{10}$$

The following transformations can be made on equation (10).

Multiplying by the inverse of $\left[K\right]$ yields

$$\left[\left[K\right]^{-1}\left[P\right] - \left[u\right]\omega^2\right]\left\{A_{mn}\right\} = 0$$

where

$$\left[K\right]^{-1}\left[P\right] = \left[D\right]$$

and $\left[D\right]$ is the dynamical matrix. The resulting equations are then in the standard form

$$\sum_{m=0}^{\infty}\sum_{n=0}^{\infty}\left[D_{mn}^{(i,j)} - \omega^2\delta_{mn}\right]\left\{A_{mn}\right\} = 0$$

where

$$\delta = 1 \quad \text{for } mn = ij$$
$$= 0 \quad \text{for } mn \neq ij$$

Since $A_{mn} = 0$ offers only the trivial solution, the problem resolves itself into the solution of the system of equations given by

$$\sum_{m=0}^{p}\sum_{n=0}^{q}\left[D_{mn}^{(i,j)} - \delta_{mn}\omega^2\right] = 0 \qquad (11)$$

where p and q equal the desired values of truncation.

It is seen that for the deflection function $w(x, y)$ chosen, equation (4) is an odd function when either m or n is odd and the other is even; and, that $w(x, y)$ is even when both m and n are either odd or even. Therefore, the equations (11) may be divided into two distinct types. Those equations which contain the nodes which are symmetrical with respect to x and y (m and n both odd or even) and those equations which contain the nodes that are antisymmetrical to x and y (m, even; n, odd: or, n, even;, m, odd). These groups of equations may be separately analyzed for solution (9).

CHAPTER III

NUMERICAL PROCEDURES

While no new computer techniques were employed, it is felt that programming of the system of equations (11) (Chapter 2) and attempts at their solution should be discussed. A program was written in FORTRAN IV language for the IBM 1050 computer for the purpose of computation and solution of these equations.

Initial attempts were aimed at computation and solution of the equations in the form of equation (10) (Chapter 2). The program input consisted of the basic plate geometry, constants, and the number of terms desired. The equations were internally computed, and the technique described by D. Young (11) and Reed (9) was employed in an attempt to find solutions. Briefly, this method of solution consisted of normalizing one of the coefficients, A_{ij}, setting the rest of the coefficients to zero, and calculating the value of ω^2. These values of ω^2 and A_{ij} were then used to recalculate ω^2, maintaining $A_{ij} = 1.0$. Using this technique, the solutions failed to converge for all values other than the fundamental.

When this scheme failed to yield satisfactory results, the program was altered to transform the computed equations to the form of equations (11) (Chapter 2), i.e., the standard eigenvalue form. The matrix operations were made using standard subroutines. Once in eigenvalue form, a standard eigenvalue root subroutine was employed in an attempt at solution. This method yielded results provided that the product of m x n was less than sixteen. Attempts to resolve this problem so that convergence could be assured were unsuccessful. It was felt that the problem occurred due to the precision of the numbers used in computation. While the eigenvalue routine was in double precision, both the equation computation and the matrix inversion techniques were single precision. A program listing is included as Appendix A.

CHAPTER IV

TEST EQUIPMENT AND TEST PROCEDURES

The resonant frequencies of two (2) test specimens were investigated. The first of these, designated specimen number 1, was a 0.1-inch thick, square plate 23.5 inches by 23.5 inches. The second, specimen number 2, was 0.1-inches thick by 11.75-inches wide by 23.5-inches long. Both specimens were 7075-T6 aluminum alloy, clad on both sides.

The specimen excitation was accomplished using a shaker system comprised of one Ling, Model 6C, shaker and one Calidyne, Model 6C, shaker. Figure 2 is a photograph of one of the shakers. Both shakers were controlled by a Calidyne excitation console, Model 77. The shakers were electrically wired so that they could be controlled either in phase, 180 degrees out of phase, or singularly. The shakers were capable of a 0.1 double amplitude displacement with a 25-pound output force when excited at 44 cps. An Altec function generator, Model 500C, was used as an input to the shaker control console. The generator had a frequency range of .01 cps to 40 kcps. The generator output was also tapped for input to a Hewlett-Packard Model 521-A frequency counter and a Chadwick Helmuth slip-sync, Model 105AR.

The Model 105AR slip-sync was used throughout testing to yield visual observation of the specimen shape. This device is essentially a stroboscope which matches the frequency of a mercury vapor lamp to the input frequency.

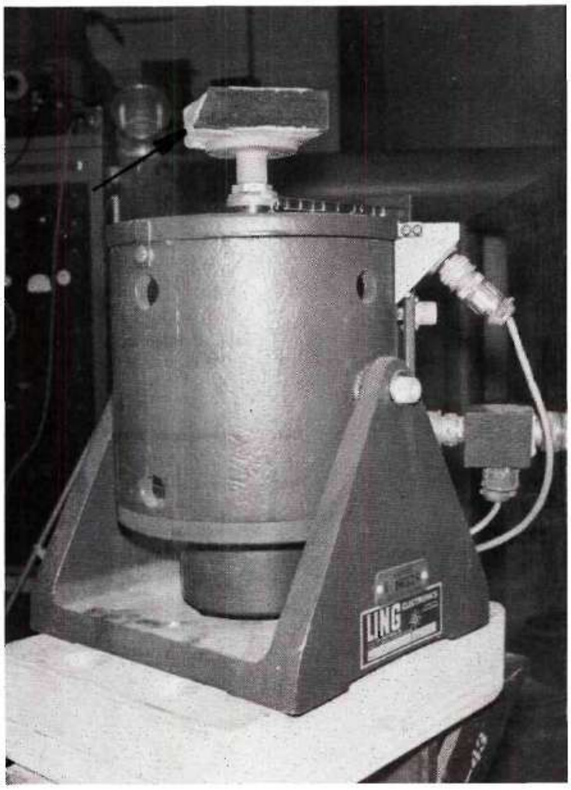

Figure 2

Model 6C Ling 25-Pound Shaker. Arrow Indicates a Sponge Rubber Pad Used to Transmit the Shaker Output

The input of the instrument could be varied such that the frequency of the mercury vapor lamp could be set less than the oscillator output frequency and the specimen vibration could be visually observed at a slow rate of vibration. Figure 3 is a photograph of the control and readout instrumentation.

Prior to use with a specimen, the shaker system frequency counter calibration was checked. The shakers were oscillated at 20 cps as indicated on the frequency counter. This was checked against a Hewlett-Packard, Model 25, stroboscope using the shaker head for the stroboscopic reference. The procedure was repeated at 100 cps. Both stroboscope and frequency counter readings at both frequencies agreed within 0.5 percent. A calibration record of 0.05 percent error is directly traceable to the National Bureau of Standards for the stroboscope.

Test specimen 1 was installed in the test support frame shown in Figure 4 by tightening the NAS 1106 bolts. These bolts were rounded to a 0.375-inch diameter to produce the desired end restraint without local crippling when tightened. The support frame and specimen were suspended from a roof truss on a chainfall. Rubber bungee chords were used at each corner of the support frame to attach the frame to the chainfall. The stiffness of the support frame and its suspension system was designed such that the natural frequency of the support system was too low to cause adverse frequency transfers between the test specimen and the support frame at the anticipated test frequencies. Figure 5 is a sketch showing the test specimen setup, and the specimen geometry is described in Figure 6.

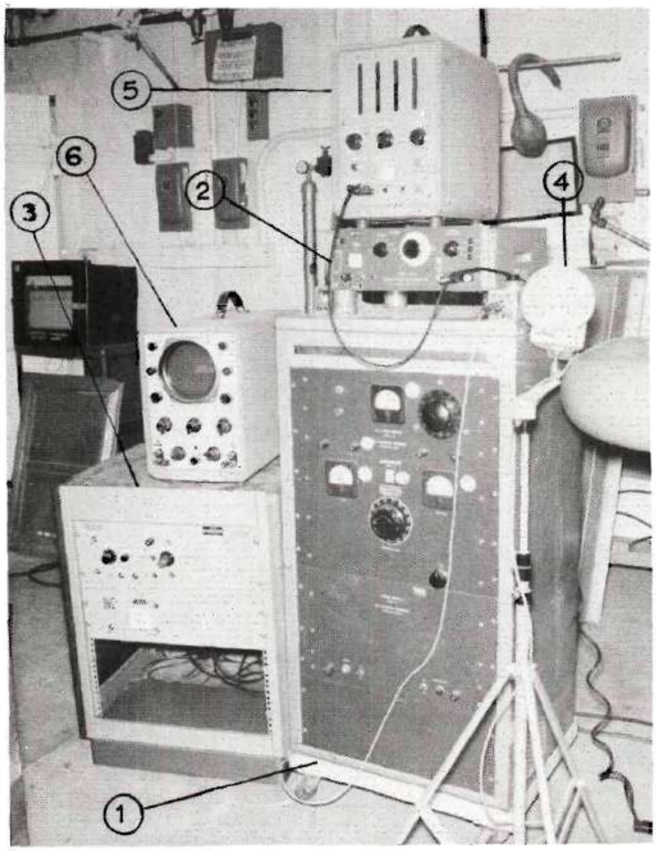

Figure 3. Control and Readout Equipment

① Calidyne Excitation Console
② Altec Function Generator
③ Chadwick Helmuth Slip-Sync
④ Mercury Lamp and Stand
⑤ Hewlett-Packard Frequency Counter
⑥ Hewlett-Packard Oscilloscope

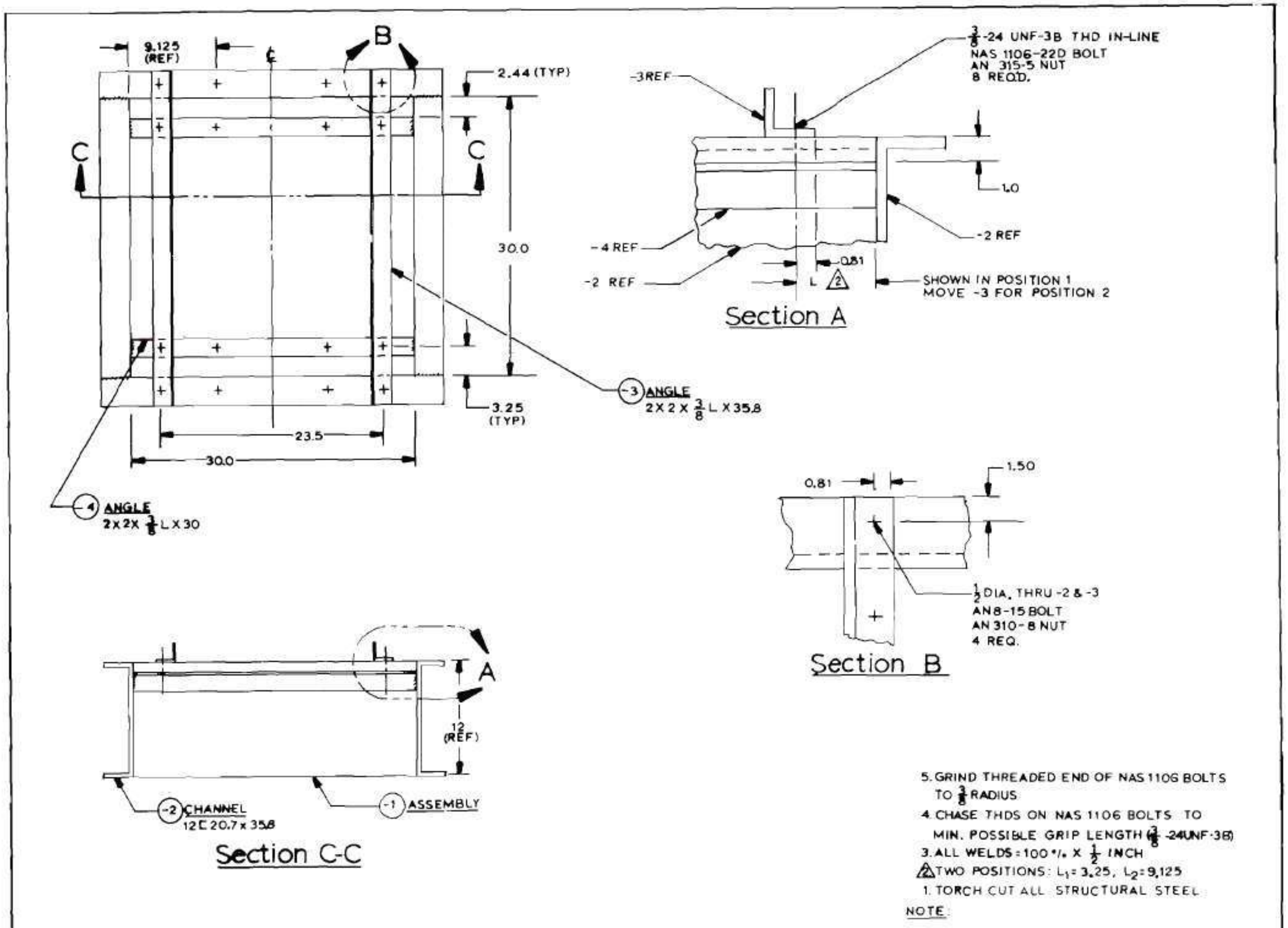

Figure 4. Test Jig

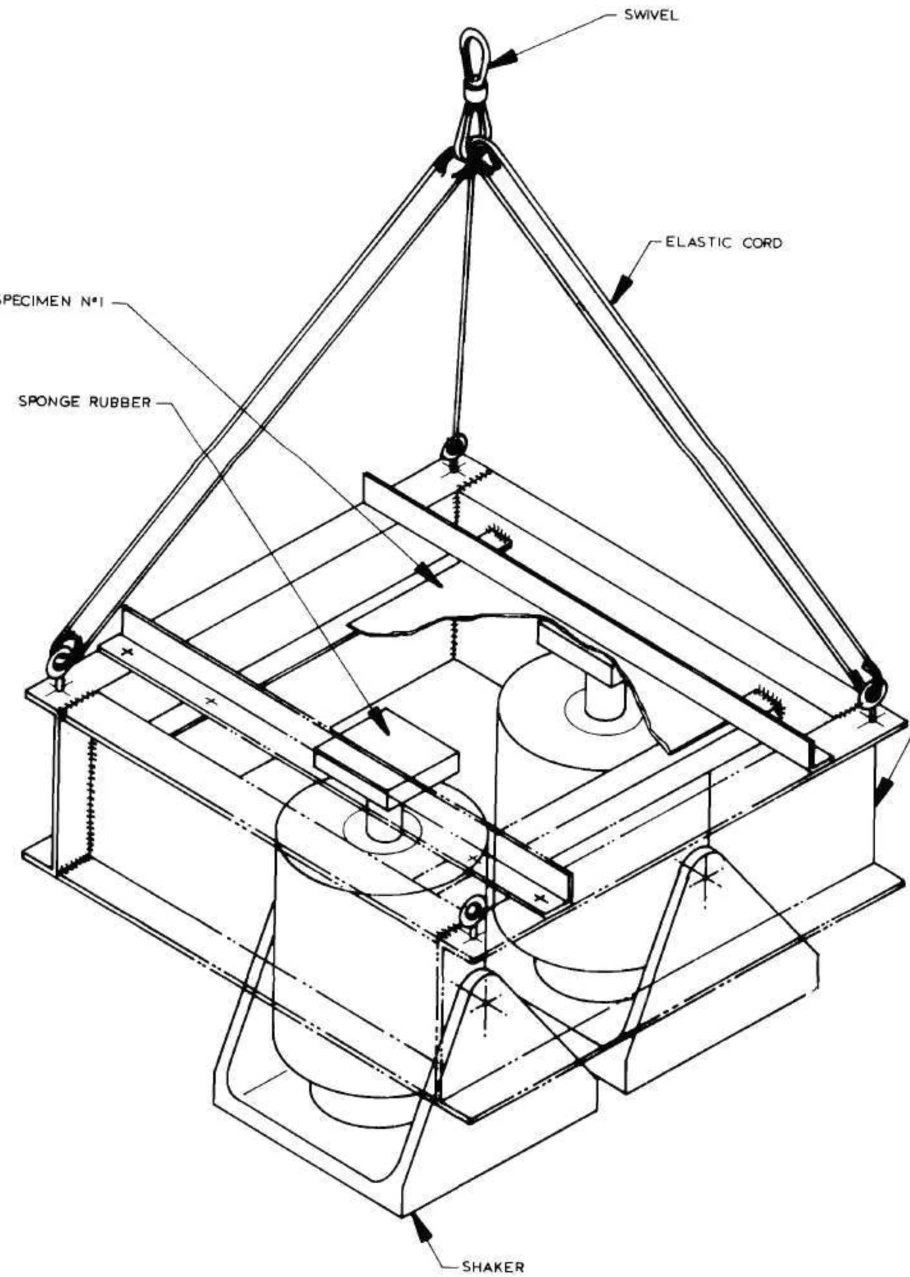

Figure 5. Test Specimen Setup

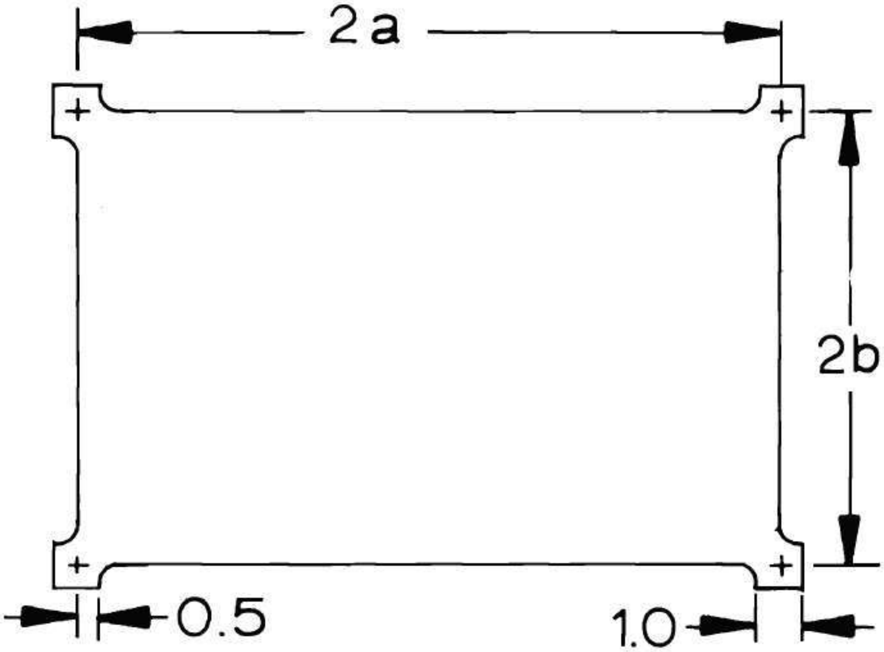

Specimen	1	2
2a	23.5	23.5
2b	23.5	11.75

Figure 6. Specimen Geometry

A 1.5 x 3 x 3-inch block of AMS3199 sponge rubber was used to attach the shaker heads to the test specimens. This rubber was wrapped with heavy duty tape which had adhesive on both sides. The bond produced by the tape was sufficient to transmit the shaker vibrations to the specimen. The shakers were attached to the quarter points, for double shaker operation, and the mid-point for single shaker operation, along the centerline of the width on both specimens.

Before testing, an intensive investigation was made to establish the "best possible" material that could be used for a "drawing" medium. The materials were evaluated on the basis of their response to the applied vibrations, their contrast for photographing, and their availability. The following materials were tested and their relative response recorded as shown below.

a) fresh coffee grounds - good

b) sugar - fair

c) used coffee grounds - good

d) sand - fair

e) hominy grits - poor

f) salt - excellent

g) black pepper - poor

h) borax - fair

i) polystyrene cubes - fair

j) polystyrene spheres - fair

k) microfine polyethelyne powder - poor

As indicated, salt gave the best results even though it was somewhat susceptible to granular cohesion at high humidities.

Testing was begun using salt as the drawing medium. The audio oscillator was set at its lowest frequency and amplitude was applied to the shakers. The salt, which had been evenly distributed on the surface of the panel, was visually observed for any lateral motion which caused salt concentrations on the panel. The frequency of the shakers was then slowly increased until a figure was drawn by local concentrations of the salt. The upper bound to the test frequency was established by the maximum output excitation force of the shakers. This procedure was repeated three times to verify the results, with the shakers operating in each of the following modes.

(1) In phase at quarter points of width centerline

(2) Out of phase at quarter points of width centerline

(3) Single shaker at mid-point of panel

The figures drawn were then photographed.

The phase relationship exhibited by the vibrating bays on the test specimen were investigated on test specimen 1 using two, hand-held MB Electronics, Type 115R, vibration pickups and a Hewlett-Packard oscilloscope, Model 103-B. A photograph of one of the pickups is shown in Figure 7. The signal from one pickup was applied to the x-axis input, while the other was applied to the y-axis input of the oscilloscope. The slope and shape of the cathode tube picture generated indicated the relative phase of the two inputs.

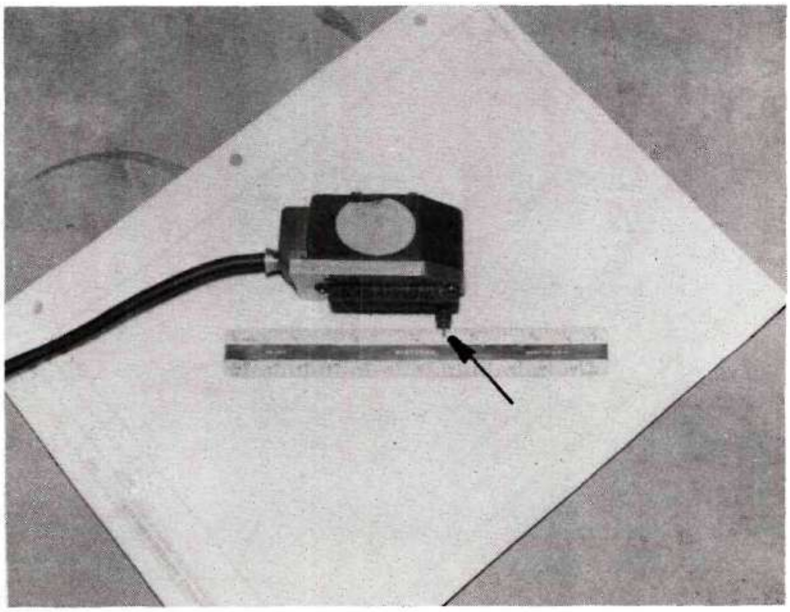

Figure 7

MB Electronics Vibration Pickup.
The Arrow Indicates Vibration Probe.

A test was conducted on specimen number 1 to insure that error was not induced due to the physical coupling of the specimen to the shaker heads. This test was performed by removal of the shaker system from the specimen and installation of a 14-inch diameter, 20-watt, Altec speaker encased in a plastic trash can. The audio output of the speaker was used to generate the exciting force in the panel. The speaker excitation was furnished by an 80-watt McIntosh amplifier, Model 240, in conjunction with the oscillator and frequency counter previously described.

The modes of specimen number 2 were established using the same methods as those of specimen number 1.

CHAPTER V

NUMERICAL SOLUTIONS AND EXPERIMENTAL RESULTS

Table 1 gives the physical properties of the two specimens tested. Table 2 and Table 3 are summaries of the calculated and experimental frequencies obtained and the method of excitation used.

Table 1. Plate Constants

	Specimen 1	Specimen 2
Material (Aluminum)	7075 T6 Clad	7075 T6 Clad
Modulus of Elasticity	10.3×10^6 psi	10.3×10^6 psi
Poisson's Ratio	0.33	0.33
Weight Density	0.1 lb per in^3	0.1 lb per in^3
Thickness	0.1 inch	0.1 inch
Length	23.5 inch	23.5 inch
Width	23.5 inch	11.75 inch

The density and modulus of elasticity used were taken from reference (12). The largest matrix considered for the Ritz solution was a 15 x 15. Photographs of the Chaldni figures obtained are given in Figures 8 through 39. The locations of the excitation shakers are indicated by arrows. In cases where the figures are nondescript, the approximate nodal lines are indicated with dotted lines. These nodal boundaries were located using vibration pickups. The experimental values

Table 2. Summary of Results, Specimen Number 1

Mode	Calculated Frequency Cps	Experimental Frequency Cps	Figure Number	Excitation Code*
1	9.24	14	8	3
	17.12			
2	34.60	26	9	2
		27	10	2
		28	11	3
3	42.96	33	12	3
4	58.31	67	13	2
5	70.54	77	14	3
		83	15	1
6	94.67	87	16	2
7	120.40	101	17	1
		104	18	2
		104	19	3
8	136.27	108	20	2
9	165.24	147	21	3
		150	22	2
10	188.69	185	23	3
		187	24	1
11	243.39	231	25	3
		236	26	1
12	375.17	316	27	3

* Excitation Code
  1 - Single Shaker
  2 - Two Shakers 180° Out of Phase
  3 - Two Shakers In Phase

Table 3. Summary of Results, Specimen Number 2

Mode	Calculated Frequency Cps	Experimental Frequency Cps	Figure Number	Excitation Code*
1	18.10	16	28	3
2	49.82	40	29	2
3	54.43	49	30	2
		50	31	1
4	93.28	99	32	2
		103	33	2
5	140.44	135	34	1
6	159.19	151	**	2
7	210.17	215	35	2
8	250.68	239	36	2
9	276.11	294	37	2
10	375.47	346	38	3
		346	39	2

*Excitation Code
1 - Single Shaker
2 - Two Shakers 180° Out of Phase
3 - Two Shakers In Phase

** This Figure was not photographed.

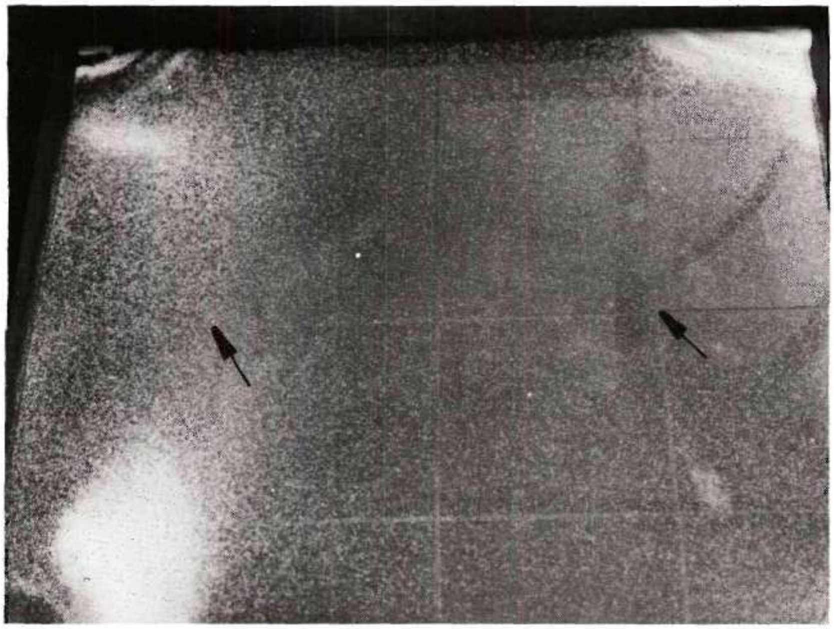

Figure 8

Specimen Number 1
Fourteen Cycles Per Second

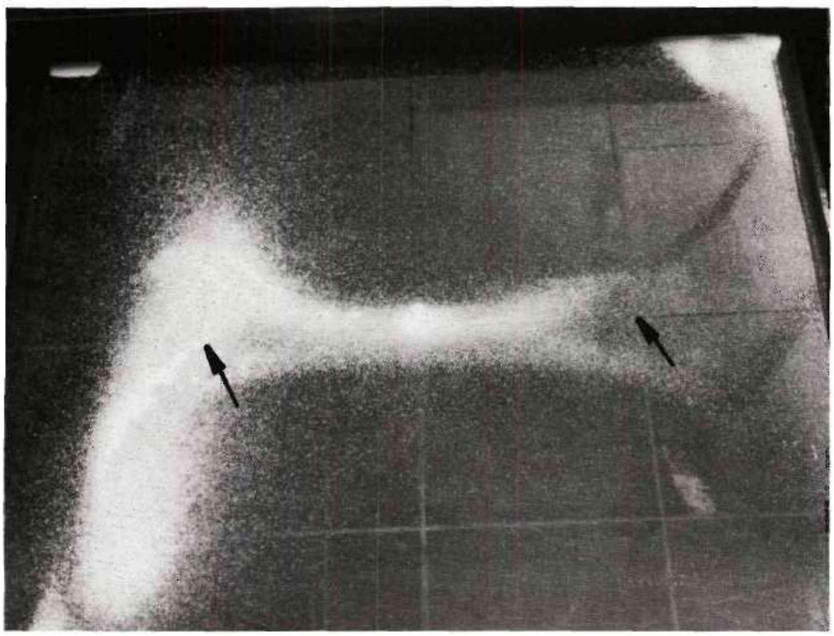

Figure 9

Specimen Number 1
Twenty-Six Cycles Per Second

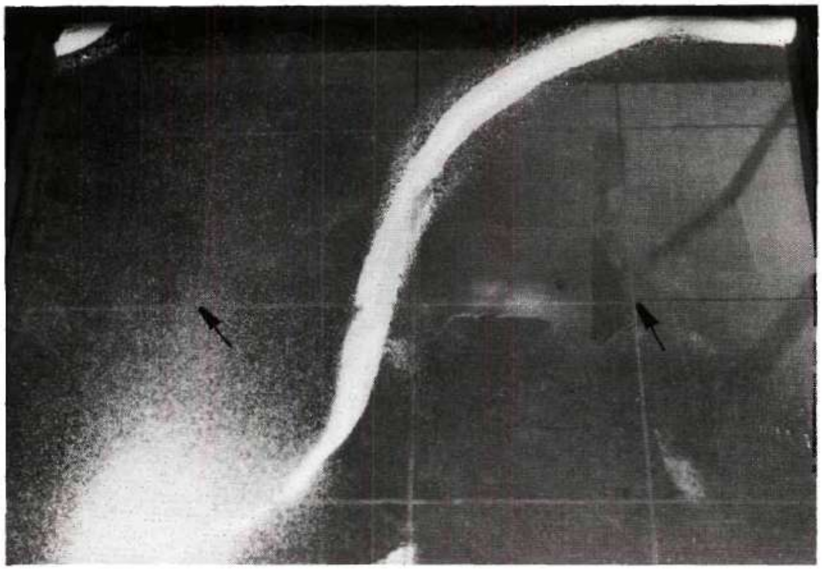

Figure 10

Specimen Number 1
Twenty-Seven Cycles Per Second

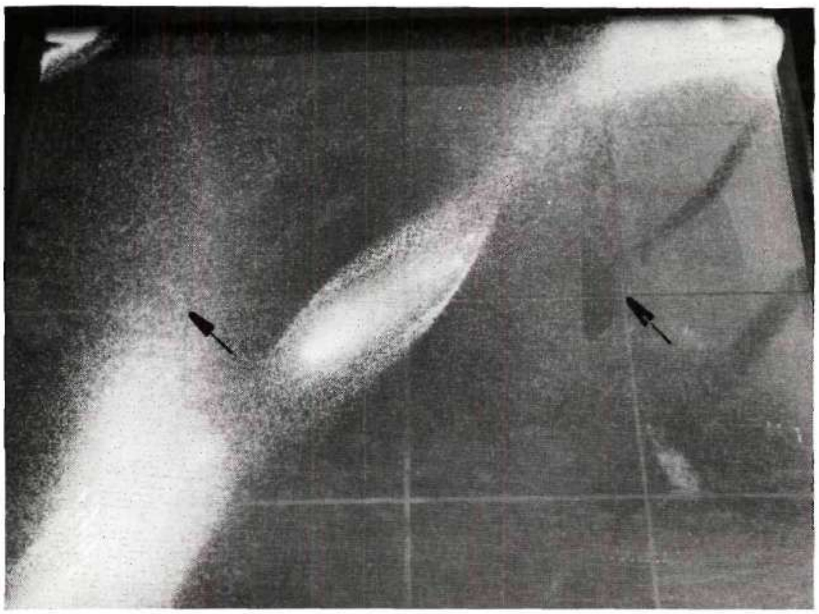

Figure 11

Specimen Number 1
Twenty-Eight Cycles Per Second

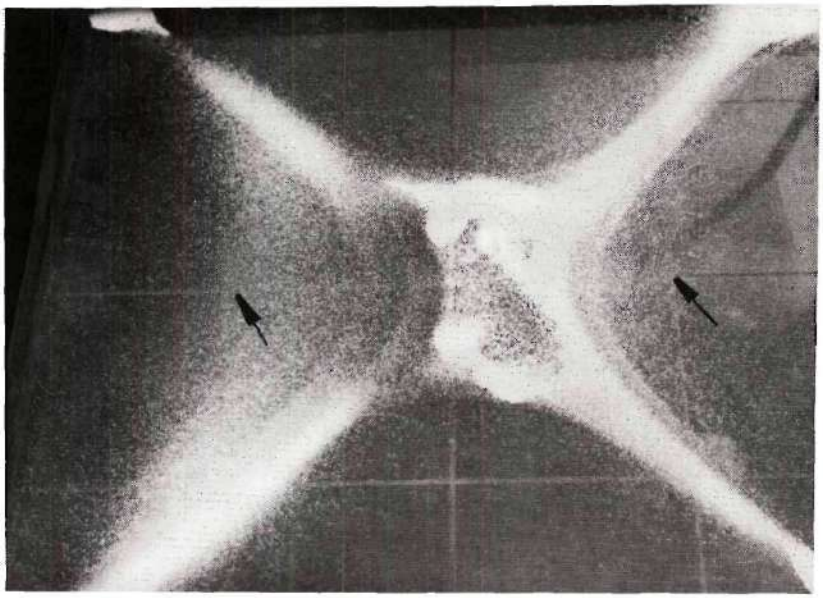

Figure 12

Specimen Number 1
Thirty-Three Cycles Per Second

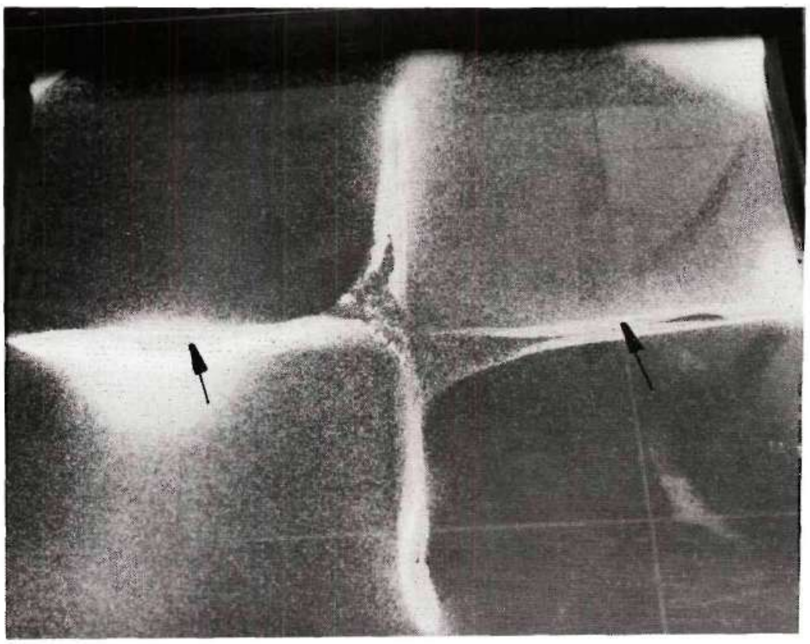

Figure 13

Specimen Number 1
Sixty-Seven Cycles Per Second

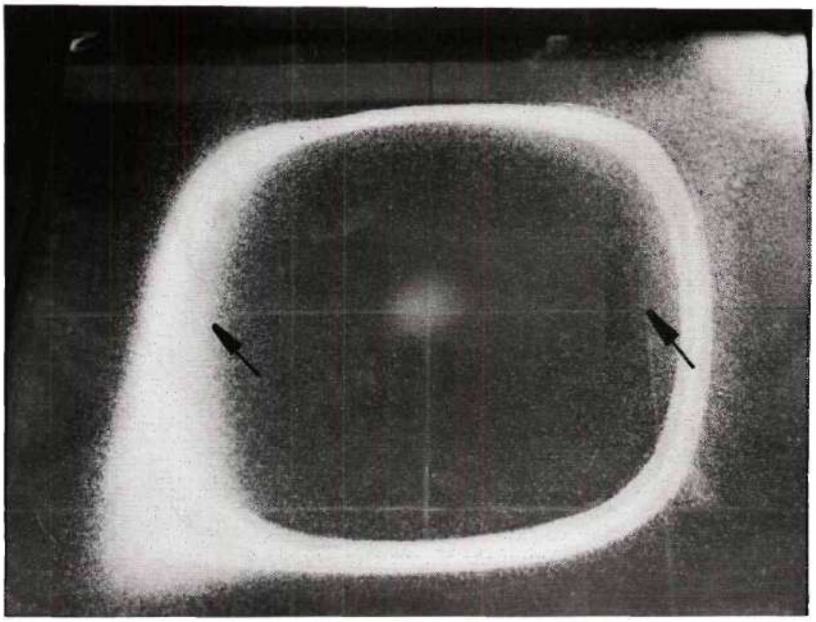

Figure 14

Specimen Number 1
Seventy-Seven Cycles Per Second

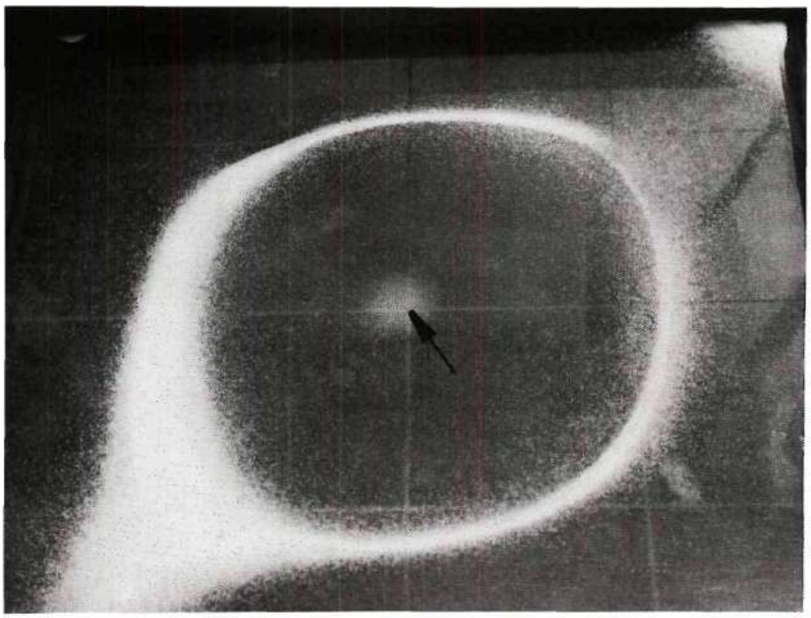

Figure 15

Specimen Number 1
Eighty-Three Cycles Per Second

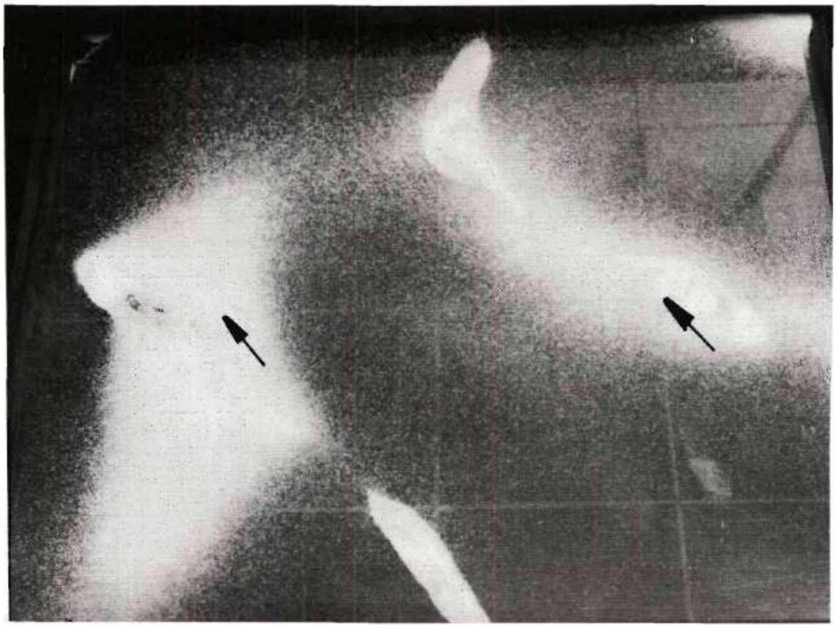

Figure 16

Specimen Number 1
Eighty-Seven Cycles Per Second

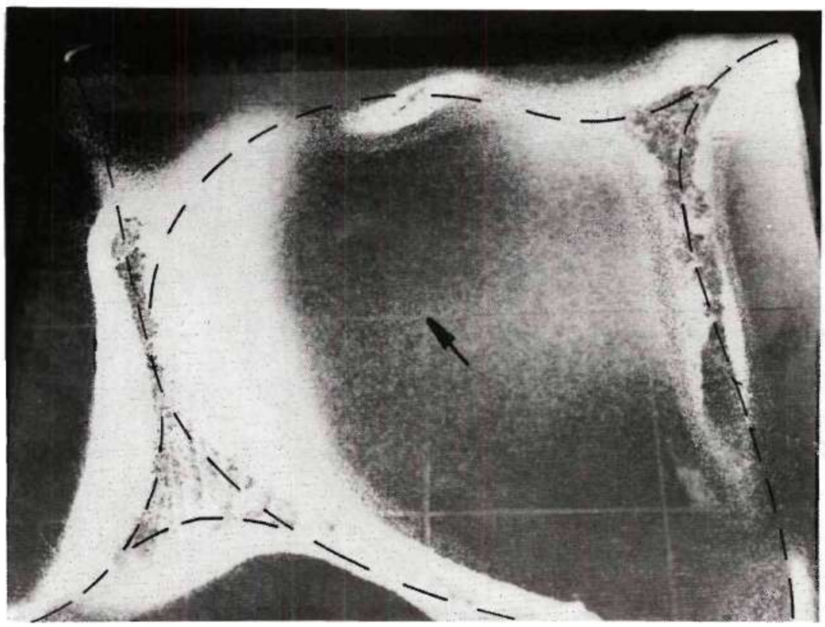

Figure 17

Specimen Number 1
One Hundred and One Cycles Per Second

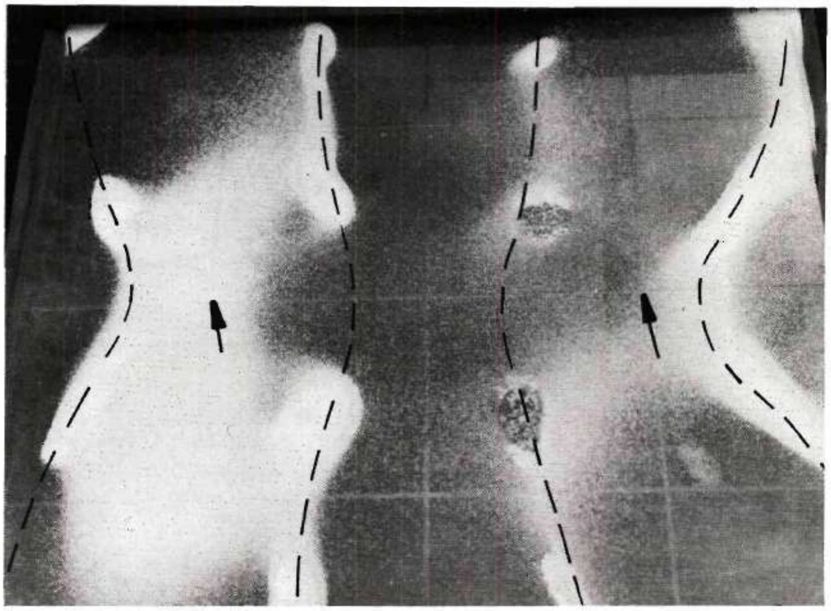

Figure 18

Specimen Number 1
One Hundred and Four Cycles Per Second

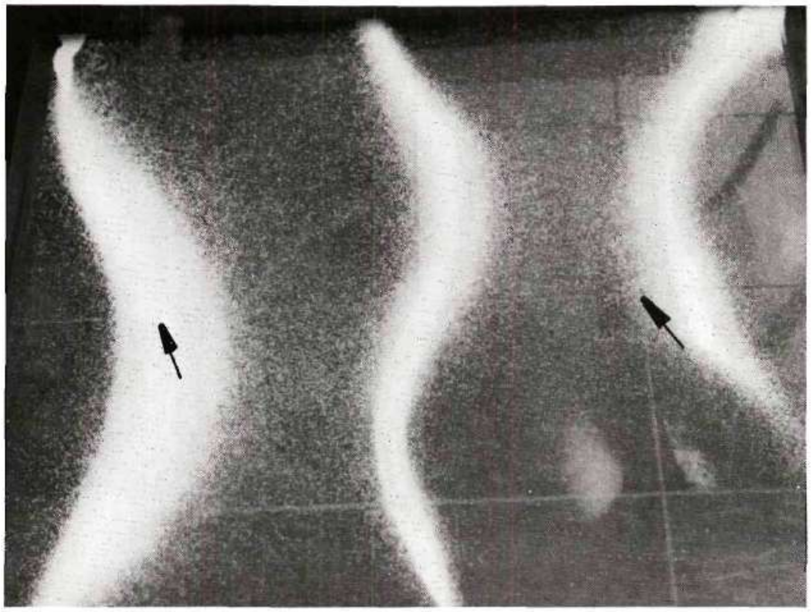

Figure 19

Specimen Number 1
One Hundred and Four Cycles Per Second

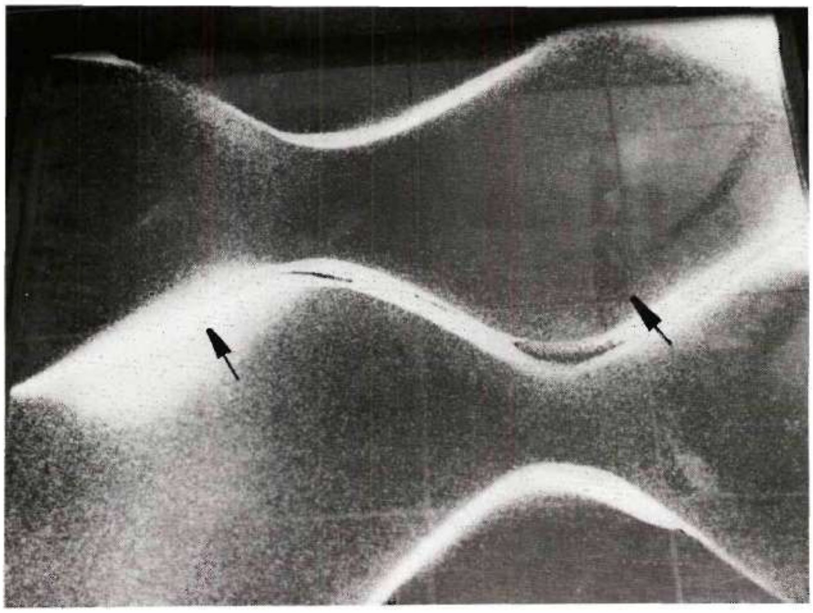

Figure 20

Specimen Number 1
One Hundred and Eight Cycles Per Second

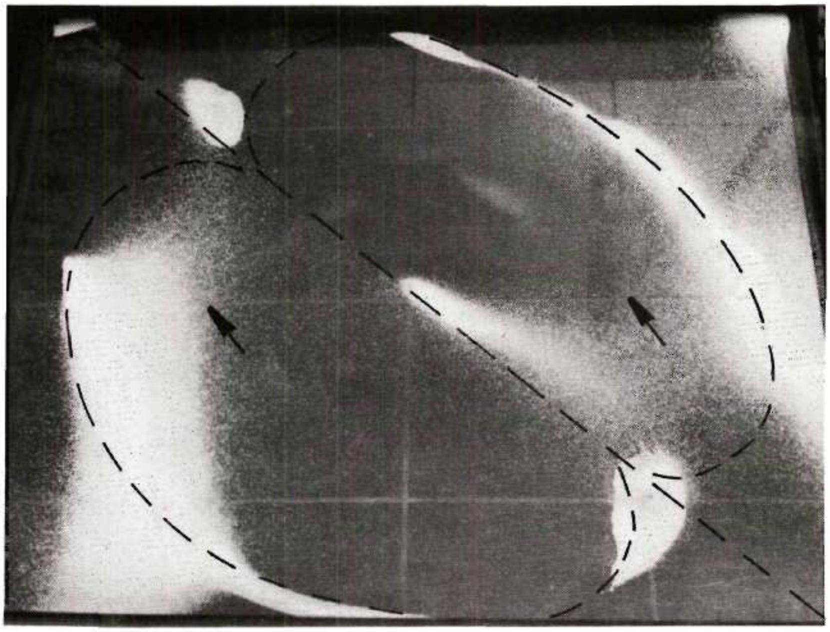

Figure 21

Specimen Number 1
One Hundred and Forty-Seven Cycles Per Second

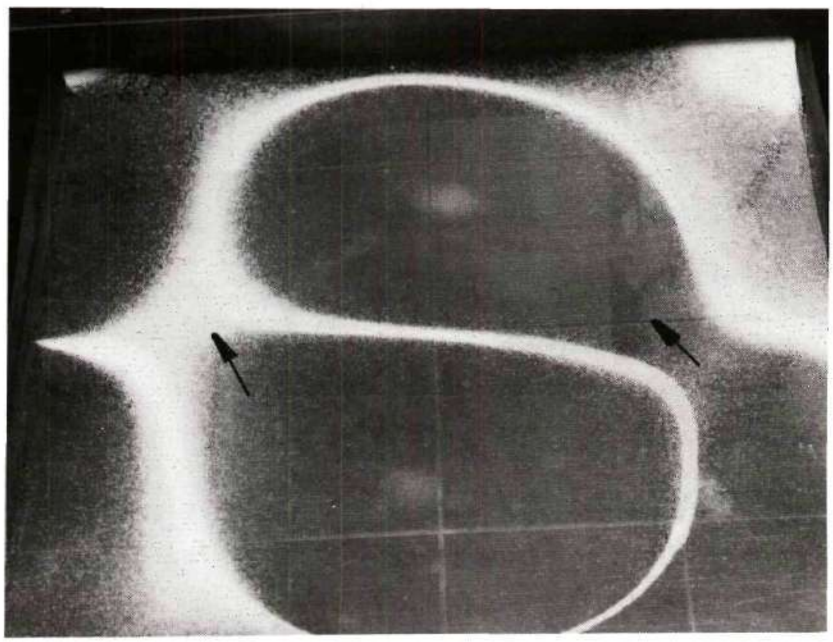

Figure 22

Specimen Number 1
One Hundred and Fifty Cycles Per Second

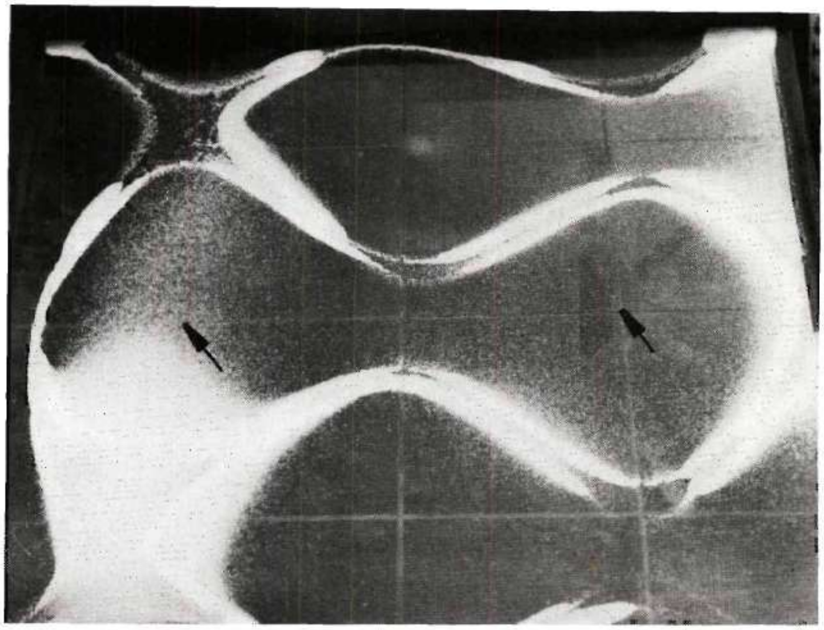

Figure 23

Specimen Number 1
One Hundred and Eighty-Five Cycles Per Second

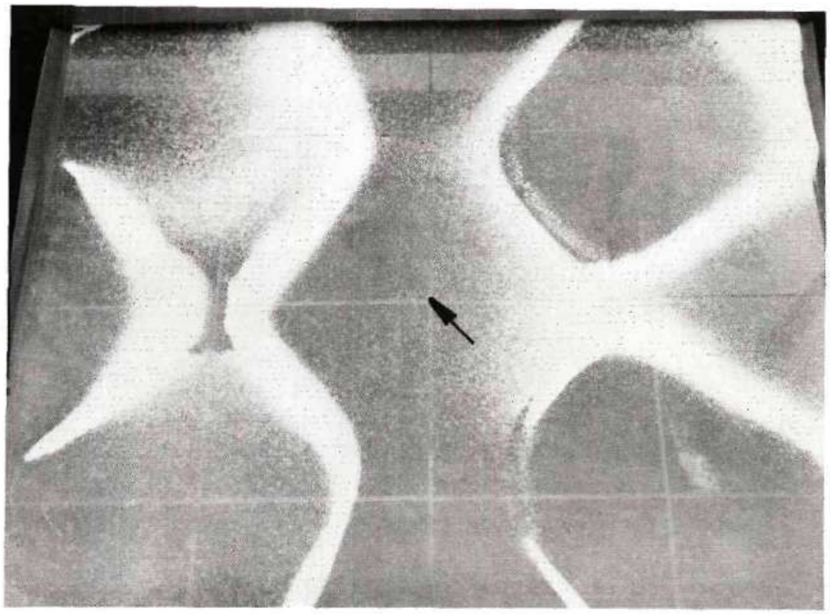

Figure 24

Specimen Number 1
One Hundred and Eighty-Seven Cycles Per Second

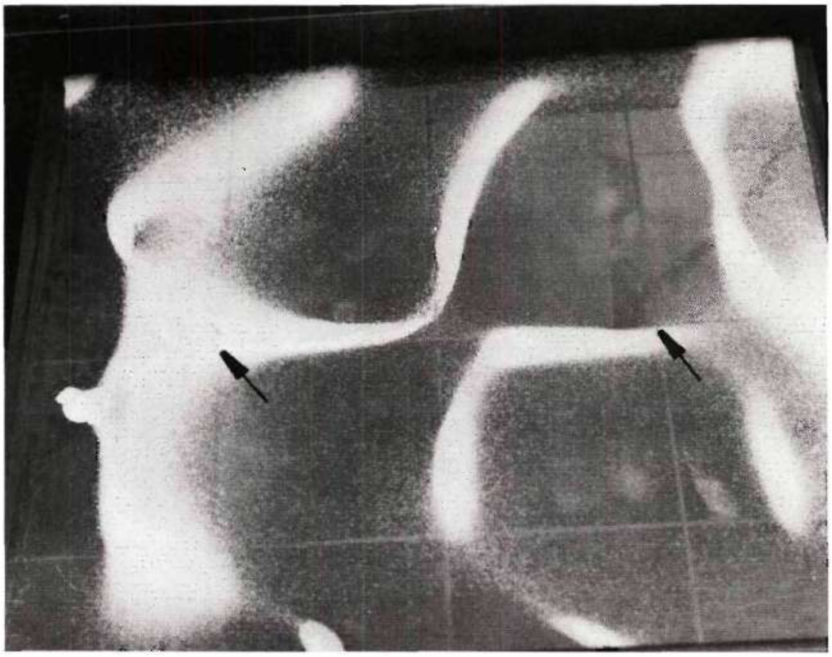

Figure 25

Specimen Number 1
Two Hundred and Thirty-One Cycles Per Second

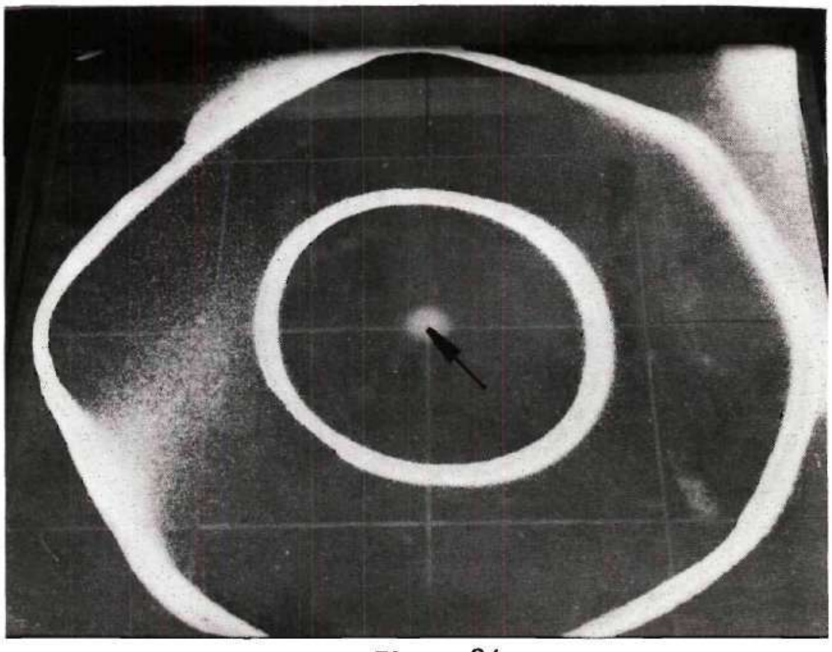

Figure 26

Specimen Number 1
Two Hundred and Thirty-Six Cycles Per Second

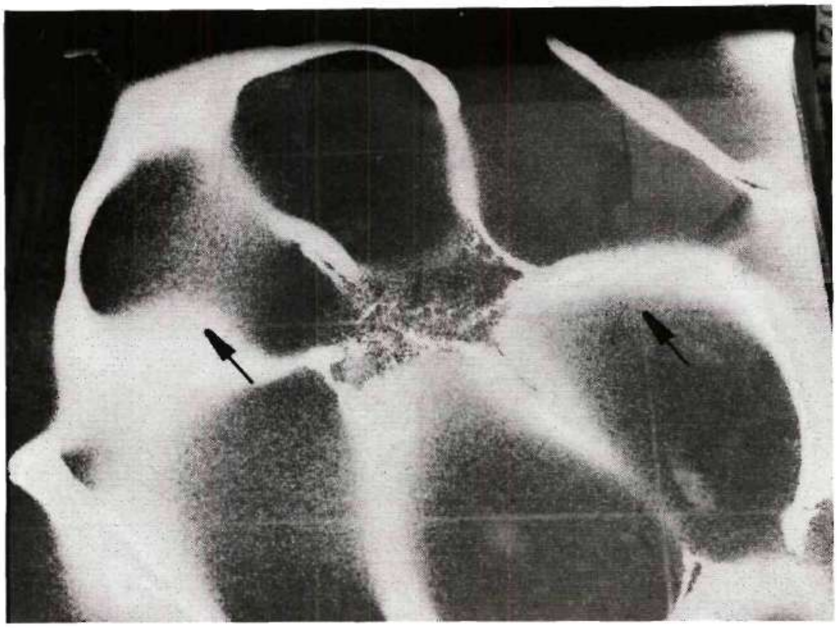

Figure 27

Specimen Number 1
Three Hundred and Sixteen Cycles Per Second

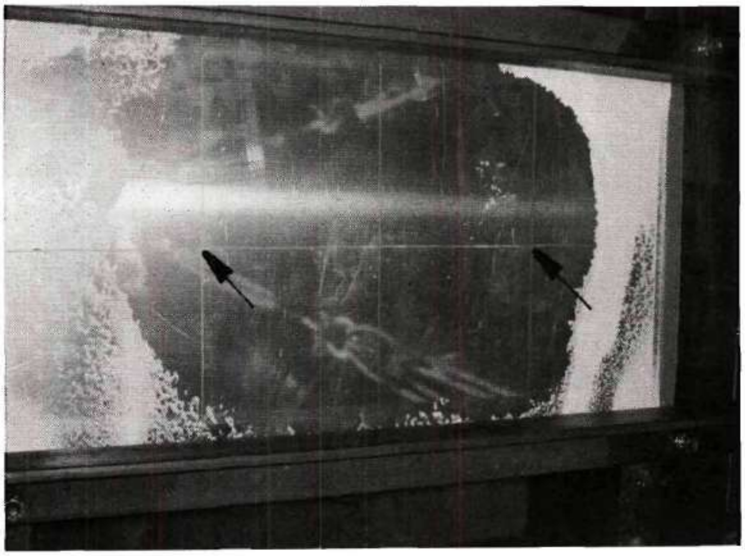

Figure 28

Specimen Number 2
Sixteen Cycles Per Second

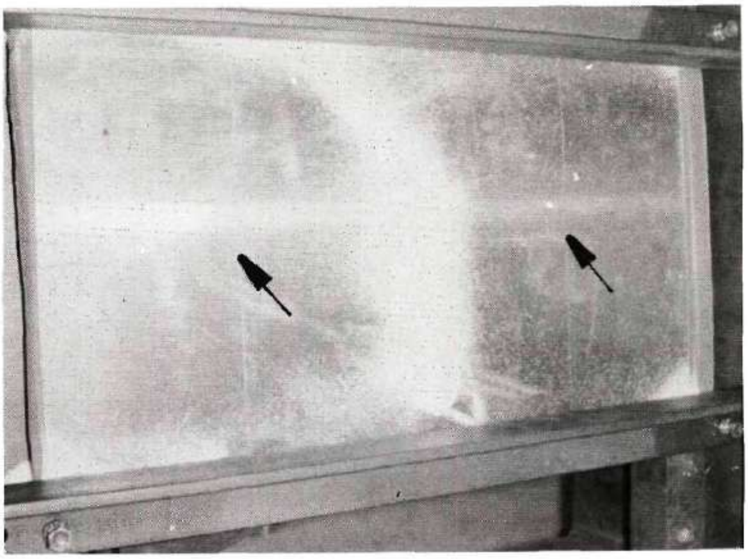

Figure 29

Specimen Number 2
Forty Cycles Per Second

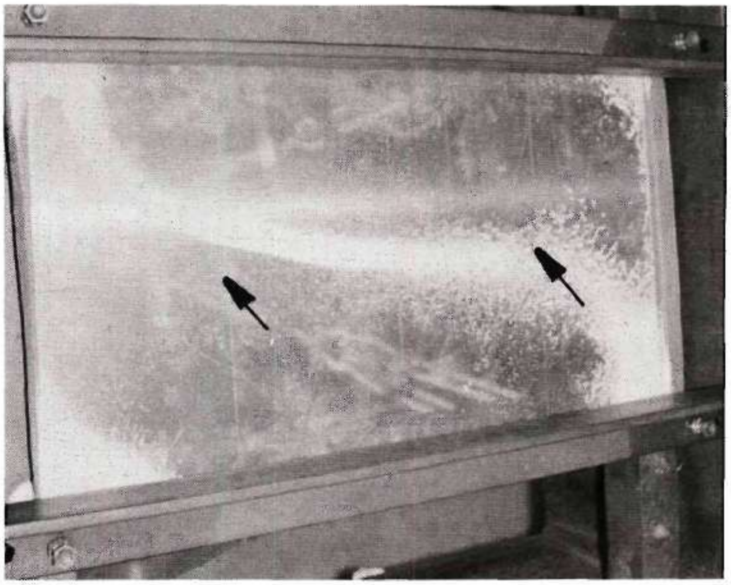

Figure 30

Specimen Number 2
Forty-Nine Cycles Per Second

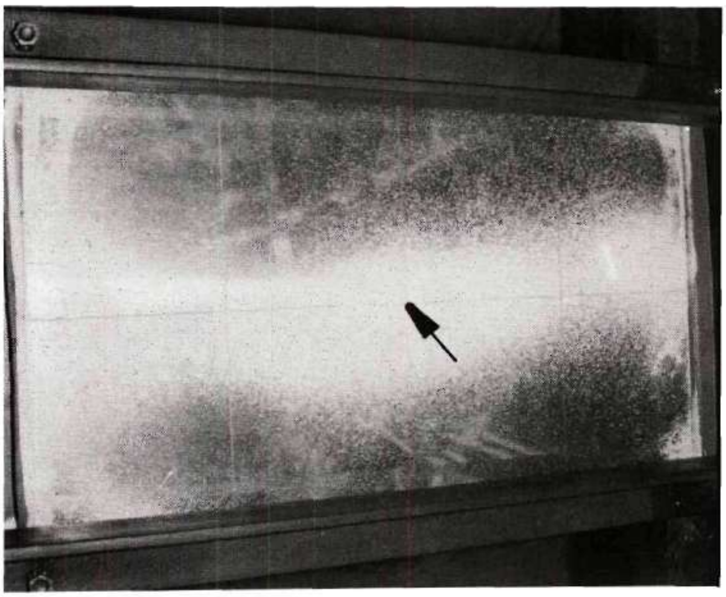

Figure 31

Specimen Number 2
Fifty Cycles Per Second

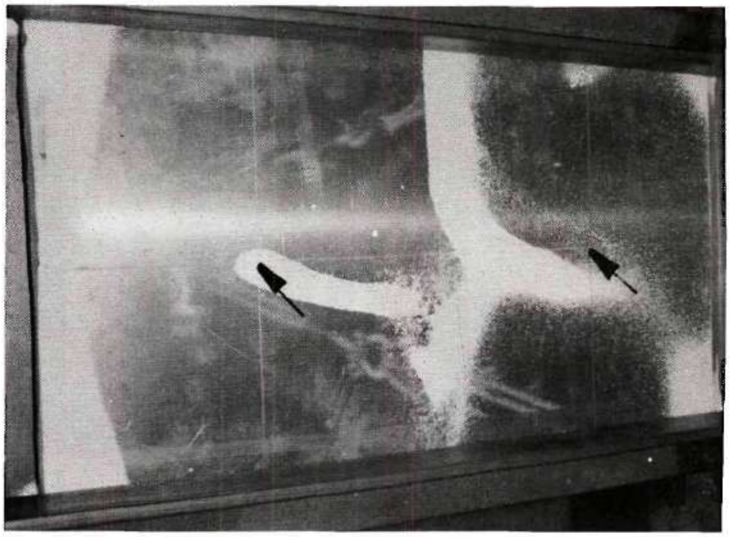

Figure 32

Specimen Number 2
Ninety-Nine Cycles Per Second

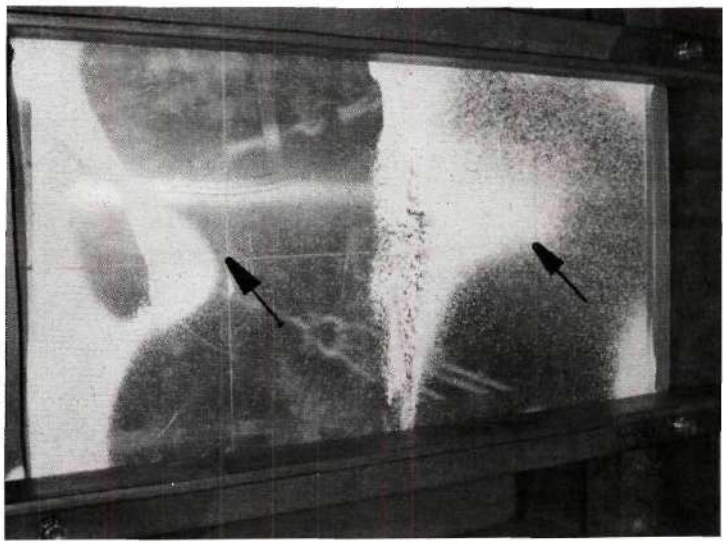

Figure 33

Specimen Number 2
One Hundred and Three Cycles Per Second

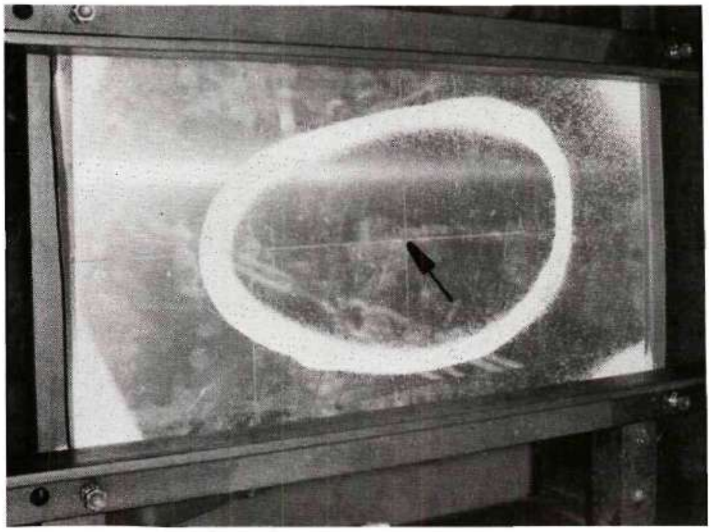

Figure 34

Specimen Number 2
One Hundred and Thirty-Five Cycles Per Second

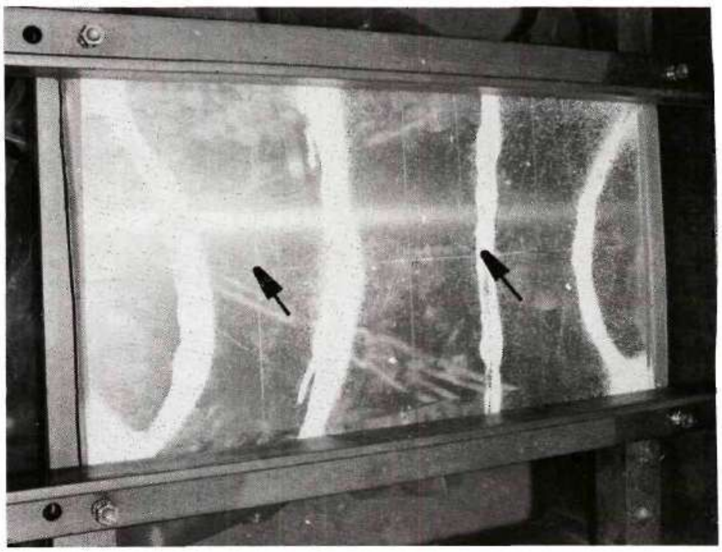

Figure 35

Specimen Number 2
Two Hundred and Fifteen Cycles Per Second

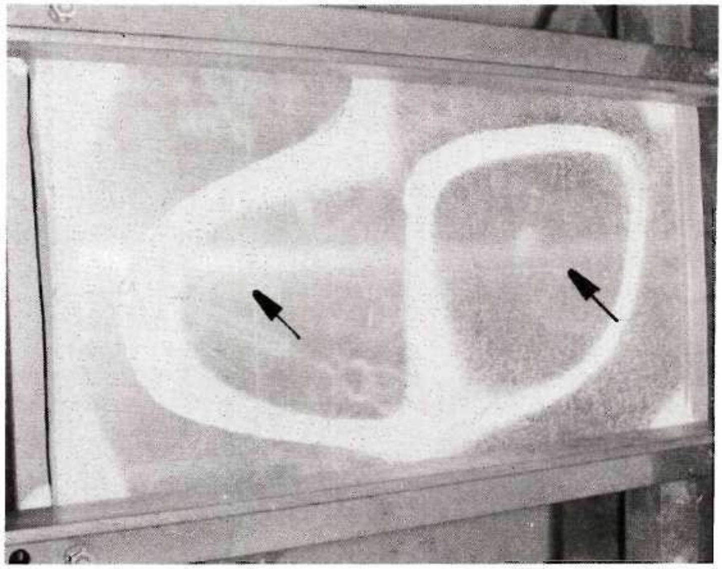

Figure 36

Specimen Number 2
Two Hundred and Thirty-Nine Cycles Per Second

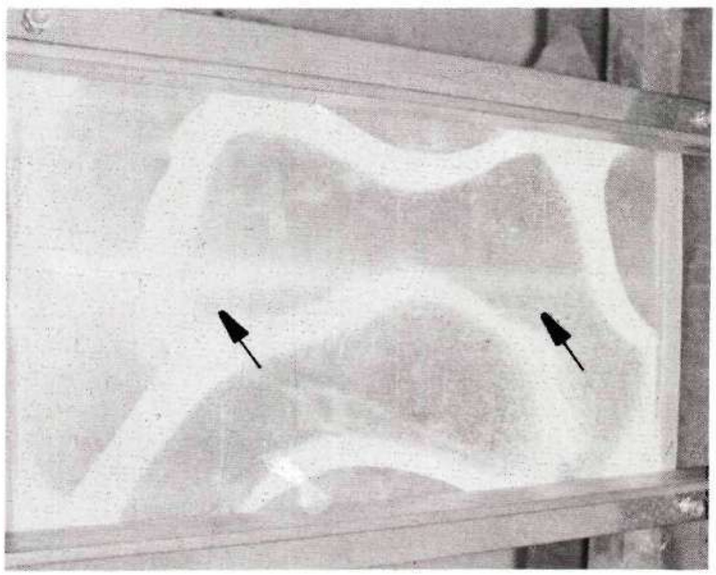

Figure 37

Specimen Number 2
Two Hundred and Ninety-Four Cycles Per Second

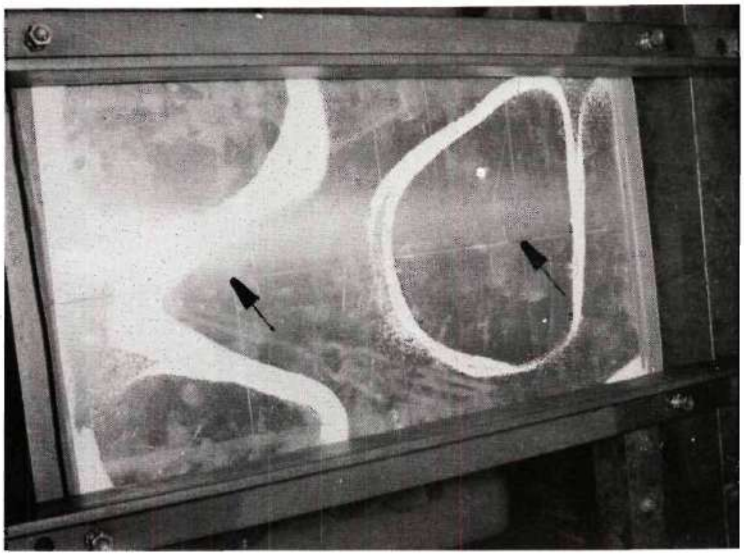

Figure 38

Specimen Number 2
Three Hundred and Forty-Six Cycles Per Second

Figure 39

Specimen Number 2
Three Hundred and Forty-Six Cycles Per Second

obtained at frequencies below 20 cps on both specimens may be in error due to violent panel responses. These large amplitude vibrations caused the drawing medium to be thrown from the panel and the resulting figures were poorly defined.

Note that the analytical solution yielded two values in the range of the fundamental for the square plate (refer to Table 2); consequently, both are presented for interpretation. A comparison of frequency constants obtained by other authors is given in Tables 4 and 5 for the square and rectangular specimens, respectively.

One extraneous root was encountered with each of the computer solutions attempted. In each case, however, the magnitude of the root was of such a low order that it was readily recognized as being extraneous.

Those verification tests using the audio output from the 20-watt Altec speaker as the driving force showed excellent correlation with regard to the frequency at which response occurred when compared to those nodes that were excited using a single shaker. Some of the figures obtained were oriented on the panel rotated 90 degrees on the plate coordinate system when compared to those obtained using a single shaker for excitation.

Table 4. Comparison of Dimensionless Frequency Parameters, k, for Square Plates

Mode Number	(1)	(2)	(3)	(4)	(5)	(6)	(7)	Figure Number (s)
1	7.46	7.12	7.12	7.68 7.44	7.8	5.44 10.10	8.3	8
2	16.80	15.77	15.73	16.54 16.74	16.8	20.33	15.4 15.9 16.6	9 10 11
3	19.60	19.60	19.13	19.94 20.17	20.6	25.34	19.5	12
4	41.46	39.33	38.42	40.62	40.7	34.36	39.5	13
5	48.26	44.42	43.55	42.76	43.1	41.55	45.4 48.9	14 15
6	51.62	50.33	---	46.07	50.8	55.81	51.3	16
7	---	---	---	67.88	67.5	70.96	59.5 61.3	17 18, 19
8	---	---	---	71.94	78.4	80.32	63.7	20
9	---	---	---	95.43	95.6	97.36	86.6 88.4	21 22
10	---	---	---	119.29	120.6	111.21	109.0 110.2	23 24

Column Legend:

(1) Reed's Analysis

(2) Reed's Experimental

(3) Cox and Boxer's Analysis

(4) Nishimura's Analysis

(5) Nishimura's Experimental

(6) Ritz Computer Solution

(7) Experimental Solution

Table 5. Comparison of Dimensionless Frequency Parameters, k, for Rectangular Plates (a/b = 2.0)

Mode Number	(1)	(2)	(3)	(4)	(5)	Figure Number
1	9.46	9.29	9.29	10.67	9.43	28
2	29.03	27.50	----	28.77	23.57	29
3	34.74	32.83	----	32.08	28.88 29.47	30 31
4	56.16	52.02	----	54.97	58.34 60.70	32 33
5	67.12	63.76	----	82.77	79.56	34
6	73.04	71.26	----	93.82	89.88	35
7	----	----	----	123.89	126.71	36
8	----	----	----	147.74	140.85	37
9	----	----	----	162.72	173.27	38
10	----	----	----	221.28	203.91	39

Column Legend:

(1) Reed's Analysis

(2) Reed's Analysis

(3) Cox and Boxer's Analysis

(4) Ritz Computer Solution

(5) Experimental Solution

CHAPTER VI

DISCUSSION OF RESULTS

The computer was utilized to give an indication as to the convergence of the answers being obtained. This was done by varying the size of the dynamical matrix up to the previously indicated maximum operational size. Indications were that although the eigenvalues being obtained were not absolute values, the rate of convergence was sufficiently low so that the values could be used as close approximations. It should be noted, however, that Reference (9) shows that when the Ritz method is used, the rate of convergence is a more accurate guide for the indication of some frequencies than it is for others. Reference (9) also indicates that even though an approximate frequency should be an upper bound, justification of the accuracy of the answer cannot be made without comparison to a known solution. In view of the above, and since known solutions are not available, the results cannot be analyzed from an error standpoint. A correlation between experimental and analytical results can be made and some insight as to the accuracy of the results can be obtained from a difference standpoint. This can best be shown in graphical form as illustrated in Figures 40 and 41, with regard to specimen 1 and specimen 2, respectively.

The manner in which the Chaldni figures are formed was apparent during testing and may be demonstrated by considering a plate in which two independent

Variation of K with Mode Number for $L_o = 1.0$

$$K_i = \frac{0.25\,\omega}{\sqrt{\left[\frac{D}{\rho H A^4}\right]}}$$

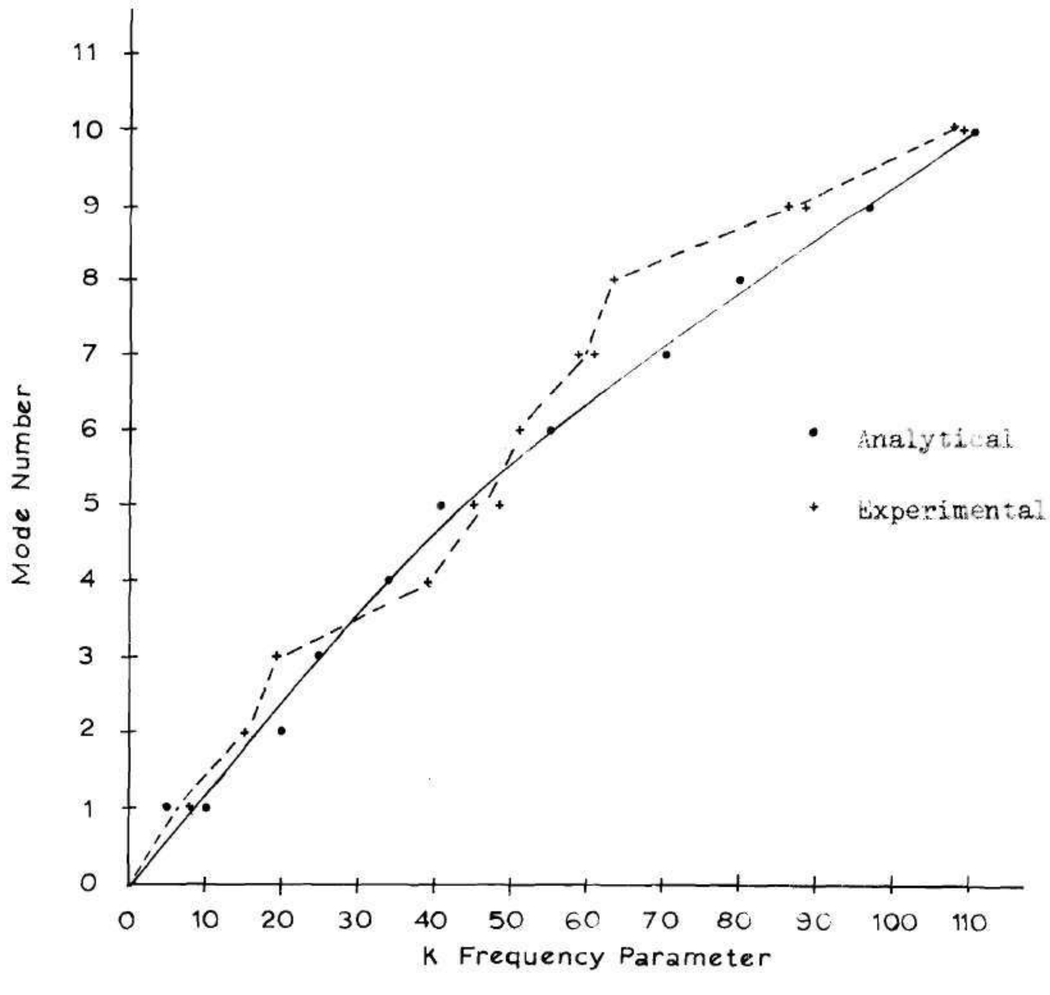

Figure 40. Comparison of Results - Specimen 1

Variation of K with Mode Number for $L_o = 2.0$

$$K_i = \frac{0.25\,\omega}{\sqrt{\left[\frac{D}{\rho H A^4}\right]}}$$

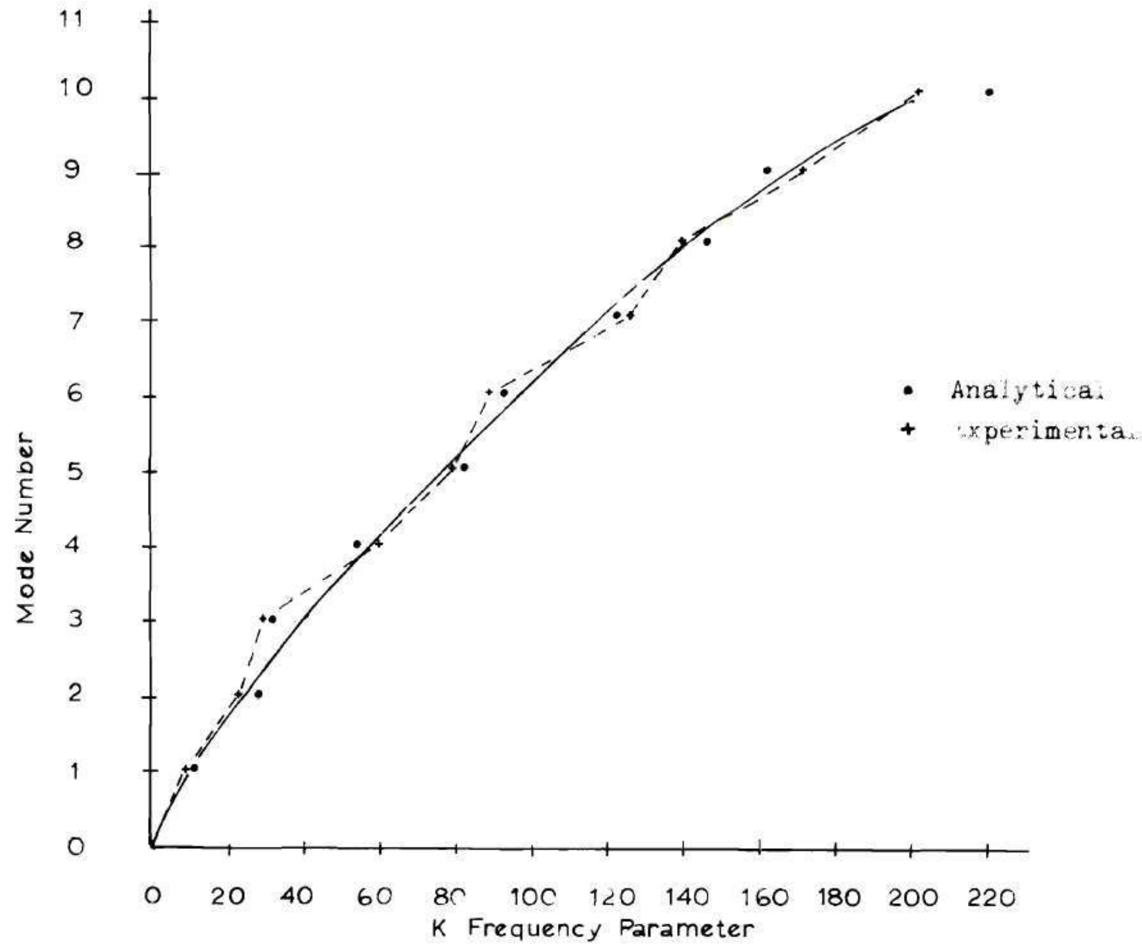

Figure 41. Comparison of Results - Specimen 2

nodes of the same frequency exist simultaneously. For example, refer to the nodal schematic in Figure 42 which represents the Chaldni figure obtained in Figure 14.

Examination of the plate when the node shape of edge A-A is superimposed on the node shape of edge B-B reveals that those areas identified by + are up and those areas identified by - are down, while those areas identified by 0 are, in some degree, stationary. The nodal lines, therefore, must pass through these 0 areas. Furthermore, they must pass through the intersections of the two separate superimposed nodes.

If the two edges are in phase with each other as shown in Figure 43 in section A-A and section B-B, investigation shows the bays to be as indicated. Since the Chaldni figure must pass through the intersections of the two superimposed nodal shapes and pass through only those bays marked with 0, it is as shown. This shape is found in Figure 12.

Through use of the Model 105AR Slip-Sync, the node shape of the edges was observed while testing. The validity of the assumption of superposition of the separate edge node shapes was verified through investigation of the nodal boundaries with hand-held vibration pickups. In some instances, the buckled bays and nodal boundaries were clearly visible during testing when the specimen was observed with a slip-sync.

It was noted during testing that the experimental values of frequencies obtained were particularly sensitive to the location of the supports, with respect to the plates, and the "flatness" of the panel being tested.

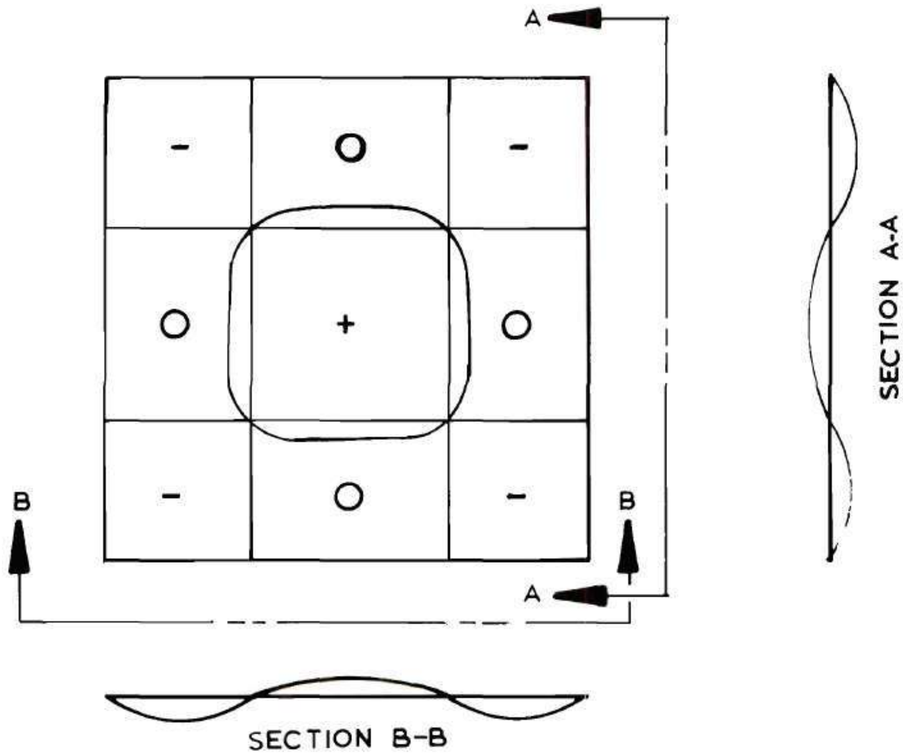

Fiqure 42. Node Formation

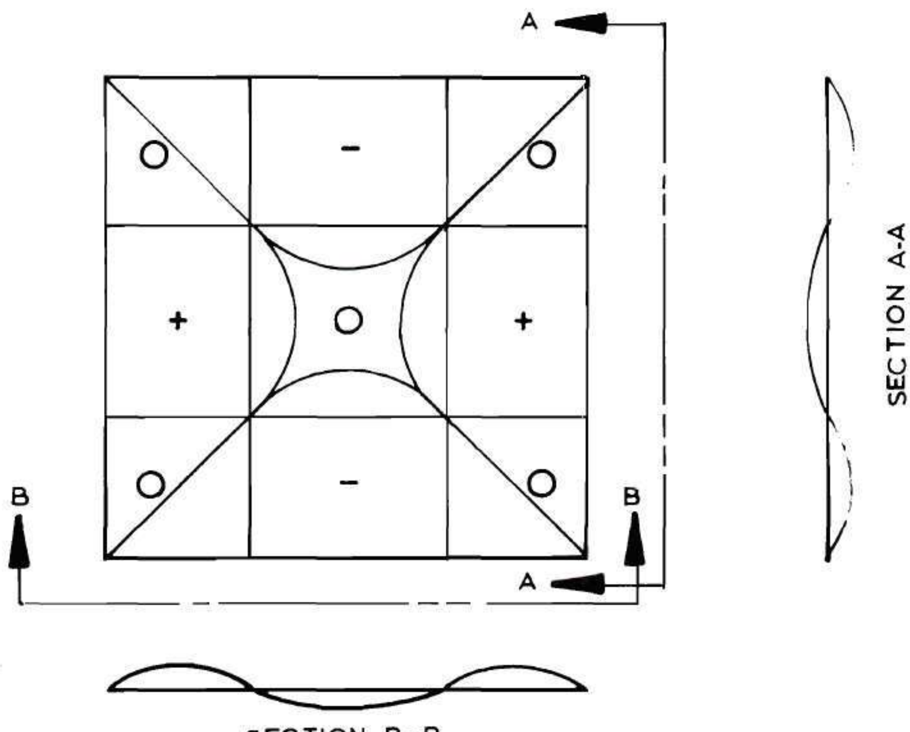

Fiqure 43. Node Formation

The agreement between the results obtained when a speaker was used for excitation in lieu of a single shaker indicated that the physical couple to the shakers used throughout the test was of minor influence on the test results. The fact that the figures formed were not always oriented on the panel in the same manner may indicate that the shakers forced the panel into a slightly higher energy mode.

CHAPTER VII

CONCLUSIONS AND RECOMMENDATIONS

The purpose of this investigation was to verify the accuracy of the deflection function (1) (Chapter 2) in predicting the natural frequencies of a vibrating plate supported by points at each of its corners, using the Ritz method. As a result of the analytical and experimental methods used, the following conclusions can be drawn.

1. The Ritz method yields equations which are readily adaptable to computer solutions, but the convergence of the solutions is hard to predict.
2. The assumed deflection equation, when analyzed using the Ritz method, yields results in the same relative order of magnitude of those found experimentally when sixteen terms are used. However, the calculated frequencies may be in error by as much as thirty-four percent on the most important mode, the fundamental.
3. Accurate experimental results can be obtained when the exciting force is physically coupled to the test specimen.
4. The resulting frequencies obtained experimentally are dependent on "exact" locations of the supports of the plate being investigated and on the initial curvature of the panel being tested.

The following recommendations are made.

1. Experimental work should be undertaken to determine the natural frequencies of plates that are point-supported at each of their corners for various other length-to-width ratios.
2. Further analytical attention should be given to the assumed deflection function to establish the frequency values at which it converges for various length-to-width ratios.

Such data are required for technological needs in designs of hatches and doorways located in high energy sound level areas.

REFERENCES

(1) Hearmon, R. F. S., "The Frequency of Vibration of Rectangular Isotropic Plates," Journal of Applied Mechanics, Volume 26, December, 1959, pages 537-540.

(2) Courant, R., "Variational Methods for the Solution of Problems of Equilibrium and Vibrations," Bulletin of the American Mathematical Society, Vol. 49, 1939, pp. 1-23.

(3) Collatz, L., "Eigenwertprobleme," Chelsea Publishing Company, New York, 1948.

(4) Grinsted, B., "Nodal Pattern Analysis," Proceedings of the Institution of Mechanical Engineers, Vol. 166, 1952, pp. 309-321.

(5) Waller, M. D., "Vibrations Produced in Bodies by Contact with Solid Carbon Dioxide," Proceedings of the Physical Society, Vol. 45, November 1932, pp. 101-115.

(6) Waller, M. D., "The Production of Chaldni Figures by Means of Solid Carbon Dioxide, Part I, Bars and Other Metal Bodies," Proceedings of the Physical Society, Vol. 49, 5, June 1937, pp. 522-530.

(7) Cox, H., and Boxer, J., "Vibration of Rectangular Plates Point-Supported at the Corners," Aeronautical Quarterly, Vol. II, Part I, February 1960, pp. 41-50.

(8) Rajappa, N., "Flexural Vibration of an Interconnected Beam System Point-Supported at the Corners," Institute of Engineers (India), December 1962, pp. 731-735.

(9) Reed, R., "Comparison of Methods in Calculating Frequencies of Corner-Supported Rectangular Plates," NASA TND-3030.

(10) Nishimura, T., "Studies on Vibrations Problems of Flat Plates by Means of Difference Calculus," Proceedings of the Third Japan National Congress for Applied Mechanics, Vol. IV-21, pp. 417-420.

(11) Young, D., "Vibration of Rectangular Plates by the Ritz Method," Journal of Applied Mechanics, Vol. 17, 1950, pp. 448-453.

(12) "Strength of Metal Aircraft Elements," Military Handbook 5, Armed Forces Supply Support Center, Washington, D. C., March 1959.

APPENDIX A

COMPUTER PROGRAM

A LISTING OF THE COMPUTER PROGRAM USED IS GIVEN BELOW FOR REFERENCE.

```
/JOB 10
C       VIPLTH CONSTANTS NO 085
        DIMENSION C1(10,10),C2(10,10),C3(10,10),C4(10,10),
       1C5(10,10),C6(10,10),C7(10,10),C8(10,10),C9(10,10),
       2D1(10,10),D2(10,10),CQ(5,5,25),CQ2(5,5,25)
       3,TM(25,25),DM(25,25),CM(25,25),AM(25,25),ROOT(25),
       4EVEC(25,25)
C       INPUT NUMR ON I3 FIELD FORMAT 101
CC      INPUT RO, H1, A, B, AND PNU ON XXX.XXX
C       INPUT K AND L ON I3 FIELD
        READ(5,601)RO,H1,A,B,PNU
  601   FORMAT(F7.4)
        READ(5,70)E
   70   FORMAT(F12.0)
  72    READ (5,101)NUMR,K,L
        OSQR=4*(RO)*(H1**3)*(1.0/386.0)
  101   FORMAT(I3)
        S=(E*(H1**3))/(12.0*(1.00-(PNU**2)))
  903   WRITE(6,503)E,S,RO,H1,A,B,PNU,K,L,NUMR
  905   CONTINUE
  503   FORMAT(1H1,F11.0,2X,F11.0,2X,5(F7.4,1X),3(I3,1X))
        L1=0
        DO 150 I=1,K
        DO 149 J=1,L
        DO 148 M=1,K
        DO 147 N=1,L
        C1(M,N)=((4.0/((M+I-1.0)*(N+J-1.0)))+(1.0/((M+I+3.0)*(N+
       1J-1.0)))+(1.0/((M+I-1.0)*(N+J+3.0)))-(4.0/((M+I+1.0)*(N
       2+J-1.0)))-(4.0/((M+I-1.0)*(N+J+1.0)))+(2.0/((M+I+1.0)*(N
       3+J+1.0)))))*1.0*A*B*OSQR
        IF(M+I-3.0)50,51,50
  50    E=1.0
        F=0.
        GO TO 52
  51    E=0.
```

```
      F=1.0
52    IF(N+J-3.0)53,54,53
53    G=1.0
      H=0.
      GO TO 55
54    G=0.
      H=1.0
55    IF(M+I-5.0)56,57,56
56    O=1.0
      P=0.
      GO TO 58
57    O=0.
      P=1.0
58    IF(N+J-5.0)59,60,59
59    Q=1.0
      R=0.
      GO TO 61
60    Q=0.
      R=1.0
61    CONTINUE
10    C2(M,N)=(H1**2)*(B/(A**3))*((I-1.0)*(I-2.0)*((M-1.0)*(M-
     12.0)*(O*(4.0/((M+I-5.0+P)*(N+J-1.0)))+(1.0/((M+I-1.0)*(N
     2+J-1.0)))+O*(1.0/((M+I-5.0+P)*(N+J+3.0)))-E*(4.0/((M+I-
     33.0+F)*(N+J-1.0)))-O*(4.0/((M+I-5.0+P)*(N+J+1.0)))+E*(
     42.0/((M+I-3.0+F)*(N+J+1.0))))+(M-1.0)*(E*(-8.0/((M+I-3.0
     5+F)*(N+J-1.0)))+E*(4.0/((M+I-3.0+F)*(N+J+1.0))))+F*(-
     64.0/((M+I-3.0+F)*(N+J-1.0)))+E*(2.0/((M+I-3.0+F)*(N+J+
     71.0)))+(2.0/((M+I-1.0)*(N+J-1.0)))+(M-1.)*(4.0/((M+I-
     81.0)*(N+J-1.0)))))
15    D2(M,N)=(H1**2)*(B/(A**3))*((I-1.0)*((M-1.0)*(M-2.0
     1)*(E*(-8.0/((M+I-3.0+F)*(N+J-1.0)))
     2+E*(4.0/((M+I-3.0+F)*(N+J+1.0))))+(M-1.0)*(16.0/((M+I-
     31.0)*(N+J-1.0)))+(8.0/((M+I-1.0)*(N+J-1.0))))+(M-1.0)*(M
     4-2.0)*(E*(-4.0/((M+I-3.0+F)*(N+J-1.0)))+(2.0/((M+I-1.0)
     5*(N+J-1.0)))+E*(2.0/((M+I-3.0+F)*(N+J+1.0))))+(8.0)*(M-
     61.0)/((M+I-1.0)*(N+J-1.0))+(4.0/((M+I-
     71.0)*(N+J-1.0)))+(I-1.)*(M-1.)*(M-2)*(4.0/((M+I-1.0
     8)*(N+J-1.0))))
20    C3(M,N)=(H1**2)*A*(1.0/B**3)*(J-1.0)*(J-2.0)*((N-1.0)*(N-
     12.0)*(Q*(4.0/((M+I-1.0)*(N+J-5.0+R)))+(1.0/((M+I-1.0)*(N
     2+J-1.0)))+Q*(1.0/((M+I+3.0)*(N+J-5.0+R)))-G*(4.0/((M+I-
     31.0)*(N+J-3.0+H)))-Q*(4.0/((M+I+1.0)*(N+J-5.0+R)))+(2.0
     4*G/((M+I+1.0)*(N+J-3.0+H))))+(N-1.0)*(G*(-8.0/((M+I-1.0
     5)*(N+J-3.0+H)))+(4.0/((M+I-1.0)*(N+
     6J-1.0)))+G*(4.0/((M+I+1.0)*(N+J-3.0+H))))-G*(4.0/((M+I-
     71.0)*(N+J-3.0+H)))+(2.0/((M+I-1.0)*(N+J-1.0)))+G*(2.0/
     8((M+I+1.0)*(N+J
     9-3.0+H))))
      C4(M,N)=((J-1.0)*((N-1.0)*(N-2.0)*(G*(-8.0/((M+I-1.0)*(N
     1+J-3.0+H)))+(4.0/((M+I-1.0)*(N+J-1.0)))+G*(4.0/((M+I+1.0
     2)*(N+J-3.0+H))))+(N-1)*(16.0/((M+I-1.0)*(N+J-1.0)))+(8.0
     3/((M+I-1.0)*(N+J-1.0))))+(N-1)*(N-2)*(G*(-4.0/((M+I-1.0)
     4*(N+J-3.0+H)))+(2.0/((M+I-1.0)*(N+J-1.0)))+(2.0/((M+I+
```

```
51.0)*(N+J-3.0+H)))*G)+8.0*(N-1.0)/((M+I-1.0)*(N+J-1.0))+
6(4.0/((M+I-1.0)*(N+J-1.0))))*(H1**2)*A*(1.0/B**3)
 C5(M,N)=((H1**2)/(A*B))*((J-1.0)*(J-2)*((M-1.0)*(M-2)*
1(E*G*(4.0/((M+I-3.0+F)*(N+J-3.0+H)))+G*(1.0/((M+I+1.0)*(
2N+J-3.0+H)))+E*(1.0/((M+I-3.0+F)*(N+J+1.0)))-G*(4.0/((M+
3I-1.0)*(N+J-3.0+H)))-E*(4.0/((M+I-3.0+F)*(N+J-1.0)))+(
42.0/((M+I-1.0)*(N+J-1.0))))+(M-1.0)*(G*(-8.0/((M+I-1.0)
5*(N+J-3.0+H)))+G*(4.0/((M+I+1.0)*(N+J-3.0+H)))+(4.0/((M
6+I-1.0)*(N+J-1.0))))+(-4.0*G/((M+I-1.0)*(N+J-3.0+H)))
7+G*(2.0/((M+I+1.0)*(N+J-3.0+H)))+(2.0/((M+I-1.0)*(
8N+J-1.0)))))
 C6(M,N)=((H1**2)/(A*B))*((J-1.0)*((M-1.0)*(M-2.0)*(
1E*(-8.0/((M+I-3.0+F)*(N+J-1.0)))+(4.0/((M+I-1.0)*(N+J-
21.0)))+E*(4.0/((M+I-3.0+F)*(N+J+1.0))))+(16.0*(M-1.0)/
3((M+I-1.0)*(N+J-1.0)))+(8.0/((M+I-1.0)*(N+J-1.0))))
4+(M-1.0)*(M-2.0)*(E*(-4.0/((M+I-3.0+F)*(N+J-1.0)))+(2.0
5/((M+I-1.0)*(N+J-1.0)))+E*(2.0/((M+I-3.0+F)*(N+J+1.0))))
6+8.0*(M-1.0)/((M+I-1.0)*(N+J-1.0))+(4.0/((M+I-1.0
7)*(N+J-1.0))))
 C7(M,N)=((H1**2)/(A*B))*((I-1.0)*(I-2.0)*((N-1.0)*
1(N-2.0)*(E*G*(4.0/((M+I-3.0+F)*(N+J-3.0+H)))+E*(1.0/((M+
2I-3.0+F)*(N+J+1.0)))+(1.0*G/((M+I+1.0)*(N+J-3.0+H)))-E*
3(4.0/((M+I-3.0+F)*(N+J-1.0)))-G*(4.0/((M+I-1.0)*(N+J-3.0
4+H)))+(2.0/((M+I-1.0)*(N+J-1.0))))+(N-1)*E*((-8.0/
5((M+I-3.0+F)*(N+J-1.0)))+E*(4.0/((M+I-3.0+F)*(N+J+1.0
6)))+(4.0/((M+I-1.0)*(N+J-1.0))))+(-4.0*E/((M+I-3.0
7+F)*(N+J-1.0)))+E
8*(2.0/((M+I-3.0+F)*(N+J+1.0)))+(2.0/((M+I-1.0)
9*(N+J-1.0)))))
 C8(M,N)=((H1**2)/(A*B))*((I-1.0)*((N-1.0)*(N-2.0)*
1(G*(-8.0/((M+I-1.0)*(N+J-3.0+H)))+(4.0/((M+I-1.0)*(
2N+J-1.0)))+G*(4.0/((M+I
3+1.0)*(N+J-3.0+H))))+(N-1.0)*((16.0/((M+I-1.0)*(N+J
4-1.0))))+(8.0/((M+I-1.0)*(N+J-1.0))))+(N-1.0)*(N-
52.0)*(G*(-4.0/((M+I-1.0)*(N+J-3.0+H)))+(2.0/((M+I-1.0
6)*(N+J-1.0)))+G*(2.0/((M+I+1.0)*(N+J-3.0+H))))+(8.0*(
7N-1.0))/((M+I-1.0)*(N+J-1.0))+(4.0/((M+I-1.0)*(N
8+J-1.0))))
 C9(M,N)=((H1**2)/(A*B))*((I-1.0)*(J-1.0)*((M-1.0)*
1(N-1.0)*(E*G*(4.0/((M+I-3.0+F)*(N+J-3.0+H)))+G*(1.0/((M+
2I+1.0)*(N+J-3.0+H)))+E*(1.0/((M+I-3.0+F)*(N+J+1.0
3)))-G*(4.0/((M+I-1.0)*(N+J-3.0+H)))-E*(4.0/((M+I-3.0+F)*
4(N+J-1.0)))+(2.0/((M+I-1.0)*(N+J-1.0))))+(N-1.0)*(
5G*(-4.0/((M+I-1.0)*(N+J-3.0+H)))+(2.0*G/((M+I+1.0)*(N+J
6-3.0+H)))+(2.0/((M+I-1.0)*(N+J-1.0))))+(M-1.0)*(E*(-4.0
7/((M+I-3.0+F)*(N+J-1.0)))+(2.0/((M+I-1.0)*(N+J-1.0)))
8+E*(2.0/((M+I-3.0+F)*(N+J+1.0))))))
 D1(M,N)=((H1**2)/(A*B))*((J-1.0)*(M-1.0)*(N-1.0)*
1(G*(-4.0/((M+I-1.0)*(N+J-3.0+H)))+G*(2.0/((M+I+1.0)*(
2N+J-3.0+H)))+(2.0/((M+I-1.0)*(N+J-1.0))))+(4*(J-1.0)
3)*(N-1.0)*G*(1.0/((M+I+1.0)*(N+J-3.0+H))))+4.0*(J-1.0
```

```
     4)*(M-1.0)*(1.0/((M+I-1.0)*(N+J-1.0)))+(I-1.0)
     5*(M-1.0)*(N-1.0)*(E*(-4.0/((M+I-3.0+F)*(N+J-1.0)))+(
     62.0/((M+I-1.0)*(N+J-1.0)))+E*(2.0/((M+I-3.0+F)*(N+J
     7+1.0))))+(4.0*(I-1.0)*(N-1.0))/((M+I-1.0)*(N+J-
     81.0))+E*(4.0/((M+I-3.0+F)*(N+J+1.0)))*(I-1.0)*(M-1.0
     9))
      C2(M,N)=(4.0*S)*((C2(M,N)+D2(M,N))+(C3(M,N)+C4(M,N))
     1+PNU*(C5(M,N)+C6(M,N)+C7(M,N)+C8(M,N))+(1.0-PNU)*
     22.0*(C9(M,N)+D1(M,N)))
      L9=L1
 147  CONTINUE
 148  CONTINUE
      L1=L1+1
      L9=L1
      GO TO (607,608,609,609),NUMR
 607      WRITE(6,504)I,J
 504  FORMAT(I3,I3)
      WRITE(6,505)((C2(M,N),C1(M,N),M,N,N=1,L),M=1,K)
 505  FORMAT(4(2H  ,F9.5,'-',F9.6,'W',I3,I3,1X))
      GO TO 149
 608  GO TO 609
 609  DO 700 M=1,K
      DO 700 N=1,L
      CQ(M,N,L1)=C1(M,N)
 700  CQ2(M,N,L1)=C2(M,N)
 149  CONTINUE
 150  CONTINUE
      GO TO (9001,9002,9003,9003),NUMR
 9002 CONTINUE
 9003 DO 9004 I=1,L1
      NUMB=0
      DO 9004 J=1,K
      DO 9004 N=1,L
      NUMB=NUMB+1
      TM(I,NUMB)=CQ(J,N,I)
 9004 DM(I,NUMB)=CQ2(J,N,I)
C      STEP 1 COMPLETE
C      INVERSION AND MULTIPLY .. STEP 2
      NN=K*L
      GO TO (9001,9009,71,71),NUMR
 9009 WRITE(6,1205)
      DO 9011 I1=1,NN
 9011 WRITE(6,300)(TM(I1,I),I=1,NN)
 71   DO 9005 I=1,NN
      XX=TM(I,I)
      TM(I,I)=1.0
      DO 9006 J=1,NN
 9006 TM(I,J)=TM(I,J)/XX
      DO 9005 K=1,NN
      IF(K-I)9007,9005,9007
```

```
 9007 XX=TM(K,I)
      TM(K,I)=0.0
      DO 9008 J=1,NN
 9008 TM(K,J)=TM(K,J)-XX*TM(I,J)
 9005 CONTINUE
      CALL MATMPY (TM,DM,CM,NN,NN,NN,25,25,25)
      GO TO (9001,22,9010,21),NUMR
 1205 FORMAT(1H1,35X,'MATRIX TO INVERT',///)
 300  FORMAT(/,4(1E18.8,2X))
  22  WRITE(6,1206)
 1206 FORMAT(1H1,35X,'POST MULTIPLIER MATRIX',///)
      DO 9012 I1=1,NN
 9012 WRITE(6,300)(DM(I1,I),I=1,NN)
      GO TO (9001,9001,9013,21),NUMR
 9010 CONTINUE
 9013 WRITE(6,1207)
 1207 FORMAT(1H1,35X,'PRODUCT MATRIX',///)
      DO 9014 I1=1,NN
 9014 WRITE(6,300)(CM(I1,I),I=1,NN)
 1007 FORMAT(1H1,///,60X,'EIGENVALUES'///(I45,E47.8//))
 1008 FORMAT(1H1///57X,'EIGENVECTOR MATRIX'///)
C STEP 2 IS COMPLETE
C BEGIN STEP 3
  21  NORM=0
        DO 9015 I=1,NN
      DO 9015 J=1,NN
 9015 AM(I,J)=CM(I,J)
      IVEC=1
      CALL ROBRAD(NN,AM,NN,IVEC,NORM,ROOT,EVEC,IND)
      IF(IND)9016,9017,9016
 9016 WRITE(6,1006)
 1006 FORMAT(////45X,'UNSATISFACTORY SOLUTION -- QUIT')
      GO TO 3000
 9017 DO 9999 J=1,NN
      IF(ROOT(J))23,25,25
 23   WRITE(6,24)J
 24    FORMAT('ROOT (',I2,') IS NEG')
      GO TO 9999
 25   ROOT(J)=.159145*(SQRT (ROOT(J)))
 9999  CONTINUE
      WRITE(6,1007)(I,ROOT(I),I=1,NN)
      WRITE(6,1008)
 3000 STOP 1111
 9001 END
       SUBROUTINE ROBRAD (NO,A,NROOT,IVEC,NORM,ROOT,EVEC,IND)
       DOUBLE PRECISION M(20,21),SUM,SOL(20),VLG
       DIMENSION A(25,25),EVEC(25,25),ROOT(25),ABC(20,21),
     1VECTOR(20),VEC(20),B(19,19),AO(20),CONS(20),
     2YVEC(20),VNEW(20),TEMP(20)
       REAL LAM,LAM1
```

```
      IND=0
      N=NO
      N1=N-1
      DO 3011 I=1,N1
3011  AO(I)=A(I,I)
      DO 3015 J=1,NO
      DO 3015 JJ=1,NO
3015  ABC(J,JJ)=A(J,JJ)
      NUM=1
 1    DO 10 I=1,N,2
      VECTOR(I)=1.
 10   VECTOR(I+1)=-1.
      NIT=1
 15   NI=1
      LAMI=0.
 20   NNUM=1
601   KEY=1
      VMAX=ABS(VECTOR(1))
      DO 6030 I=2,N
      V1=ABS(VECTOR(I))
      IF(V1-VMAX)6030,6030,6020
6020  VMAX=V1
      KEY=I
6030  CONTINUE
      DO 6050 I=1,N
      VEC(I)=0.
      IF(VECTOR(KEY))6040,6050,6040
6040   VEC(I)=VECTOR(I)/VECTOR(KEY)
6050     CONTINUE
      IF(NNUM-5)6100,6100,7000
6100  CONTINUE
      DO 6070 I=1,N
      VECTOR(I)=0.
      DO 6070 J=1,N
6070  VECTOR(I)=VECTOR(I)+A(I,J)*VEC(J)
      NNUM=NNUM+1
      GO TO 601
7000  ZDENC=0.
      ZNUM=0.
      DO 7010 I=1,N
      ZDENC=ZDENC+VECTOR(I)**2
7010  ZNUM=ZNUM+VEC(I)*VECTOR(I)
     LAM=0.
     IF(ZNUM)7020,7030,7020
7020  LAM=ZDENC/ZNUM
7030  DIFF=LAM-LAMI
     PER=0.
     IF(LAM)7040,7050,7040
7040  PER=ABS(DIFF/LAM)
7050  IF(PER-.1E-5)1000,1000,50
```

```
50      IF(NI-3)60,60,200
60      LAMI=LAM
        NI=NI+1
        DO 70 I=1,N
70      VECTOR(I)=VEC(I)
        GO TO 20
200     IF(NIT-7)210,1700,1700
210     NIT=NIT+1
        GO TO 15
1700    IND=1
        GO TO 3200
1000    ROOT(NUM)=LAM
       IF(NUM-1)1500,1010,1500
1010    DO 1020 J=1,N
1020    EVEC(J,1)=VEC(J)
        GO TO 1510
1500    IF(NUM-NROOT)1510,3000,3000
1510    NUM=NUM+1
        DO 1520 I=1,N
1520    VECTOR(I)=VEC(I)
        NMAX=1
        RX=ABS(VECTOR(1))
        DO 8020 I=2,N
        SX=ABS(VECTOR(I))
        IF(SX-RX)8020,8010,8010
8010    NMAX=I
        RX=SX
8020    CONTINUE
        XMAX=VECTOR(NMAX)
        DO 8030 I=1,N
       VNEW(I)=0.
       IF(XMAX)8025,8030,8025
8025    VNEW(I)=VECTOR(I)/XMAX
8030    CONTINUE
        IF(N-NMAX)8040,8070,8040
8040    DO 8050 I=1,N
        TEMP(I)=A(I,NMAX)
        A(I,NMAX)=A(I,N)
8050    A(I,N)=TEMP(I)
        DO 8060 I=1,N
        TEMP(I)=A(NMAX,I)
        A(NMAX,I)=A(N,I)
8060    A(N,I)=TEMP(I)
8070    N1=N-1
        VNEW(NMAX)=VNEW(N)
        DO 8100 I=1,N1
        DO 8100 J=1,N1
8100    B(I,J)=A(I,J)-VNEW(I)*A(N,J)
        N=N-1
        IF(N-1)1525,1600,1525
```

```
1525  DO 1530 I=1,N
      DO 1530 J=1,N
1530  A(I,J)=B(I,J)
      GO TO 1
1600  ROOT(NUM)=B(1,1)
3000  IF(IVEC)3200,3010,3200
3010  N1=NO-1
      DO 3005 I=1,N1
3005  CONS(I)=0.
      DO 3100 L=2,NROOT
      DO 3020 J=1,N1
3020  ABC(J,J)=AO(J)-ROOT(L)
      CONS(NO)=ROOT(L)
      NN1=NO+1
      DO 9010 I=1,NO
9010  ABC(I,NN1)=CONS(I)
      DO 9015 I=1,NO
      DO 9015 J=1,NN1
9015  M(I,J)=ABC(I,J)
      DO 9020 I=1,NO
9020  M(I,1)=ABC(I,1)
      DO 9030 I=2,NN1
      IF(ABC(1,1))9030,9025,9030
9025  M(1,I)=0.
      GO TO 9037
9030  M(1,I)=ABC(1,I)/ABC(1,1)
9037  I1=1
      J2=2
      K1=0
      DO 9200 II=2,NO
      I1=I1+1
      J1=J2
      J2=J2+1
      K1=K1+1
      DO 9050 I=I1,NO
      SUM=0.
      DO 9040 K=1,K1
9040  SUM=SUM+M(I,K)*M(K,J1)
9050  M(I,J1)=M(I,J1)-SUM
      DO 9070 J=J2,NN1
      SUM=0.
      DO 9060 K=1,K1
9060  SUM=SUM+M(I1,K)*M(K,J)
9070  M(I1,J)=M(I1,J)-SUM
      DO 9080 J=J2,NN1
      IF(M(I1,I1))9999,9075,9999
9075  M(I1,J)=0.
      GO TO 9080
9999  M(I1,J)=M(I1,J)/M(I1,I1)
9080  CONTINUE
9200  CONTINUE
```

```
       SOL(NO)=M(NO,NN1)
      NN2=NO-1
      JJ=NO
      DO 9300 II=2,NO
      JJ=JJ-1
      SUM=0.
      K1=NN1
      DO 9250 K=JJ,NN2
      K1=K1-1
 9250 SUM=SUM+M(JJ,K1)*SOL(K1)
      SOL(JJ)=M(JJ,NN1)-SUM
 9300 CONTINUE
      IF(NORM)300,300,301
 300  VLG=DABS(SOL(1))
      NOPE=1
      DO 302 J=2,NO
      IF(VLG-DABS(SOL(J)))303,302,302
 303  NOPE=J
      VLG=DABS(SOL(J))
 302  CONTINUE
      GO TO 310
 301  NOPE=NORM
 310  DO 3030 J=1,NO
     EVEC(J,L)=0.
     IF(SOL(NOPE))3025,3030,3025
 3025 EVEC(J,L)=SOL(J)/SOL(NOPE)
 3030 CONTINUE
 3100 CONTINUE
 3200 RETURN
      END
/DATA
/END
```